Development of Frequency Controlled Ionic Polymer Metal Composite (IPMC) Microactuator for Drug Delivery Application

CHANG XI LIANG

A project report submitted in partial fulfilment of the requirements for the award of Bachelor of Engineering (Hons.) Electrical & Electrical Engineering

Lee Kong Chian Faculty of Engineering and Science
Universiti Tunku Abdul Rahman

Agust 2017

DECLARATION

I hereby declare that this project report is based on my original work except for citations and quotations which have been duly acknowledged. I also declare that it has not been previously and concurrently submitted for any other degree or award at UTAR or other institutions.

Signature : _____

Name : CHANG XI LIANG

ID No. : 1307298

Date : 28/8/2017

APPROVAL FOR SUBMISSION

I certify that this project report entitled **"DEVELOPMENT OF FREQUENCY CONTROLLED IONIC POLYMER METAL COMPOSTE (IPMC) MICROACTUATOR FOR DRUG DELIVERY APPLICATION"** was prepared by **CHANG XI LIANG** has met the required standard for submission in partial fulfilment of the requirements for the award of Bachelor of Electrical & Electronic Engineering at Universiti Tunku Abdul Rahman.

Approved by,

Signature : _____

Supervisor : Dr Chee Pei Song

Date : _____

ACKNOWLEDGEMENTS

I would like to thank everyone who had contributed to the successful completion of this project. I would like to express my gratitude to my research supervisor, Dr. Chee Pei Song for his invaluable advice, guidance and his enormous patience throughout the development of the research.

In addition, I would also like to express my gratitude to UTAR lab facilities assistants for their generous effort for providing the lab facility.

ABSTRACT

Wireless microactuators offer many application opportunities. One of the promising applications is for implantable drug delivery devices, which allow site-specific drug administration. These devices allow drugs to be delivered at a targeted location to increase drug efficiency in order to combat targeted disease such as osteoporosis treatment, chronic ocular disease, and pain control. In comparison to early approaches of battery powered and active circuitry drug delivery device, this passive operation mechanism eliminates the need for active circuitry and batteries and is thus advantageous in term of size, cost, longevity, and robustness. Ionic polymer metal composite (IPMC), operates at low voltage with the capability of large stimulus strain production, appears to be a promising actuator candidate to control over drug delivery rate. The microactuator can be controlled through frequency manipulation which further benefits the programmable drug schedule, and wireless drug release. In this thesis, a wireless drug delivery device with planar magnetic coupling resonant wireless power (MCR-WPT) transfer system and frequency controlled IPMC microactuator was deconstructed. IPMC serve as microactuator that driven by the passive *L-C* resonant circuit that generate output voltage by tuning the field frequency to the resonant frequency of the circuit. The planar *L-C* resonant circuits were fabricated with etching technique to have the resonant frequency of 13.56MHz, which were coupled with IPMC microactuator on the PDMS device body. The fabricated *L-C* resonant circuits provide 1.89V at it resonant, causing 0.77mm defection of the IPMC microactuator. The time response of the IPMC microactuator was experimentally demonstrated, which shown that it has a fast response.

TABLE OF CONTENTS

DECLARATION **ii**
APPROVAL FOR SUBMISSION **iii**
ACKNOWLEDGEMENTS **v**
ABSTRACT **vi**
TABLE OF CONTENTS **vii**
LIST OF TABLES **x**
LIST OF FIGURES **xi**
LIST OF SYMBOLS / ABBREVIATIONS **xiii**

CHAPTER

1 INTRODUCTION **1**
1.1 Background 1
1.2 Problem Statement 2
1.3 Aims 2
1.4 Objectives 2
1.5 Scope and Limitation of the Study 2

2 LITERATURE REVIEW **3**
2.1 Background Study 3
2.2 Ionic Polymer Metal Composite 4
2.3 Load Carrying Capability of IPMC Actuator 6
2.4 Wireless Implantable Drug Delivery Devices 7
2.4.1 One-time Release Based Drug Delivery Device 8
2.4.2 Multiple-Time Release Based Drug Delivery Device 10
2.5 Summary of Literature Review 12
2.6 Related Theory 13

	2.6.1	Resonant Frequency	13
	2.6.2	Magnetic Resonance Coupling (MRC)	14
3	**METHODOLOGY AND WORK PLAN**		**15**
3.1	Design Scheme		15
	3.1.1	Design Phase	16
	3.1.2	Fabrication Phase	17
	3.1.3	Data Collection phase	18
3.2	Device Design and Working Principle		19
3.3	Fabrication		21
	3.3.1	Planar L-C circuit	21
	3.3.2	Device Body	25
	3.3.3	IPMC Microactuator	29
3.4	Class-E Amplifier & Rectifier Circuit		32
	3.4.1	Class E amplifier	32
	3.4.2	Rectifier Circuit	34
	3.4.3	Summary of Methodology	36
4	**RESULTS AND DISCUSSION**		**37**
4.1	Wireless Drug Delivery Device Using IPMC Actuator		37
4.2	Resonance Response & Distance Response of the MCR-WPT Prototype		38
	4.2.1	Resonant Response	39
	4.2.2	Distance Response	41
4.3	Effect on Asymmetrical MRC-WPT		42
4.4	Time response of the IPMC micro-actuator		44
5	**RESULTS AND DISCUSSION**		**46**
5.1	Conclusion		46
5.2	Future Improvement		46
REFERENCES			**47**

APPENDICES **50**

LIST OF TABLES

Table	TITLE	PAGE
Table 3.1:	Coefficient value of the planar print spiral coil	23
Table 3.2:	Characteristics value of transmitter and receiver	23
Table 3.3:	Silver mirror process solution mixing ratio	31
Table 3.4:	Calculated characteristic value for class E amplifier	33
Table 3.5:	Proposed characteristic value for class E amplifier	33
Table 3.6:	Proposed characteristic value for rectifier circuit	35
Table 4.1:	Theoretical vs Experimental	40
Table A-1:	DC Voltage vs Field Frequency	50
Table A-2:	DC Voltage vs Distance	51
Table A-3:	DC Voltage vs Angle of rotation	51

LIST OF FIGURES

FIGURE	TITLE	PAGE
Figure 2.1:	Operation principle of IPMC	4
Figure 2.2:	Force couple model for IPMC actuator	6
Figure 2.3:	A frequency controlled wireless implantable drug delivery device using hydrogel microactuator	8
Figure 2.4:	A frequency sensitive wireless SMP actuator	9
Figure 2.5:	A wireless implantable drug delivery with hydrogel microvalves	10
Figure 2.6:	A IPMC actuated valvelss pump for drug delivery	11
Figure 2.7:	Resonant Frequency	13
Figure 2.8:	Conceptual view of Magnetic Resonance Coupling	14
Figure 3.1:	An overview of the project work plan	15
Figure 3.2:	An overview of the workflow during design phase	16
Figure 3.3:	An overview of the workflow during fabrication phase	17
Figure 3.4:	An overview of the workflow during data collection phase	18
Figure 3.5:	Drug delivery device with frequency-controlled wireless IPMC microactuator	19
Figure 3.6:	Block diagram of the wireless prototype drug delivery device with IPMC microactuator	20
Figure 3.7:	Concept view of the planar print spiral coil: (a) square (b) hexagon (c) octagonal (d) circular	21
Figure 3.8:	(a) Fabricated 11x11mm Receiver Planar *L-C* resonant circuit. (b) Fabricated 100x100mm Transmitter Planar *L-C* resonant circuit.	25
Figure 3.9:	The dimension of the prototype IDDs device body	26
Figure 3.10:	The transparent view of prototype device body	27

Figure 3.11: Mould created using resin based 3D printer 27

Figure 3.12: The designed mould of the wireless IDDs device 28

Figure 3.13: The transparent view of the designed mould 28

Figure 3.14: Fabricated prototype device body using IPMC 29

Figure 3.15: Dimension of the T-shape IPMC microactuator 30

Figure 3.16: Complete fabricated IPMC microactuators through silver mirror process 31

Figure 3.17: Schematic diagram of the class-E amplifier 32

Figure 3.18: Fabricated Class-E Amplifier 34

Figure 3.19: Schematic Diagram of the Rectifier Circuit 34

Figure 4.1: (a.) Experimental Setup For Resonance Response, (b.) Separation Distance, *D* Is Varied to Study Distance Response 39

Figure 4.2: DC Voltage vs Field Frequency 39

Figure 4.3: DC Voltage vs Separation Distance 41

Figure 4.4: Asymmetrical Effect Experimental Setup 42

Figure 4.5: DC Voltage vs Angle of rotation 43

Figure 4.6: Time Response & Defection Experimental Setup 44

Figure 4.7: DC Voltage vs Deflection vs Time 45

LIST OF SYMBOLS / ABBREVIATIONS

L	inductance, H
C	capacitance, F
ω	angular resonant frequency
Q	quality factor
φ	impedance angle of filter branch, º
R	resistance, Ω
f_r	resonance frequency, Hz
φ	fill factor
d_{avg}	average diameter
D_{out}	outer diameter, mm
D_{in}	inner diameter, mm
C_n	coefficient expression for planar print spiral coil
K_n	coefficient expression for planar print spiral coil
W	width, mm
S	spacing, mm
n	number of turn
D	separation distance, cm
IPMC	ionic polymer metal composite
MRC	magnetic resonance coupling
IDDs	implantable dug delivery device
MCR-WPT	magnetic coupled resonance Wireless Power Transfer
PDMS	polydimethylsiloxane
EAP	electroactive polymer
SMA	shaped memory alloy
SMP	shaped memory polymer
AC	alternative voltage
DC	direct voltage
L-C	inductor-capacitor
MEMS	Micro-Electro-Mechanical Systems

CHAPTER 1

INTRODUCTION

1.1 Background

Micro-Electro-Mechanical Systems (MEMS) for drug delivery applications have attracted significant interests that have led to extensive investigations (Tsai, and Sue, 2007). The purpose of implantable MEMS devices for drug delivery applications are to provide specific-site controllable drug release through miniaturized devices and offer more effective therapies (Sarraf, Wong, and Takahata, 2011). Wireless MEMS drug delivery devices that operate with passive control circuitry for release triggering and control eliminate the need of batteries. This provide advantages in terms of size, cost, and complexity of the device. Lot of efforts have developed for passively operated wireless microactuators, but not all of them are suitable for implant drug delivery applications due to issues related to the high voltages requires and lack of controllability (Rahimi, and Takahata, 2011).

Ionic polymer metal composites (IPMC) is a type of electroactive polymer used as both sensors and actuator for biomedical drug delivery application. This novel smart material is responsive to voltage. IPMC act operates as a flexible actuator when a voltage is applied across it in a cantilever configuration (Andrew, et.al., 2011). IPMC has lend themselves well to miniaturization and suitable to be used as microactuator in the wireless power system for a drug delivery device, which can operate in low voltage.

This thesis reports a frequency controlled wireless IPMC microactuator based on inductor-capacitor (*L*-*C*) planar resonant circuit for drug delivery application. The actuation technique also potentially extends for biomedical application.

1.2 Problem Statement

Traditional intake such as oral or injection of drugs for patients is extremely low efficient and not ideal as the dosage is not stable overtime. The efficiency of the drug delivery device operate with physical batteries also may be limited due to the size of the batteries and may causes more risk to the patient such as batteries leakage, remove for rechargable, and etc. A solution to this is to develop a drug delivery device that can be operated wirelessly.

1.3 Aims

This research aims to develop IPMC microactuator operated using frequency controlled wireless approach. In addition, the wireless power transfer mechanism-magnetic coupling will be the subject of study on how the power transfer efficiency affect the IPMC performance and the feasibility in drug delivery device.

1.4 Objectives

In order to achieve the aim for this research, three main set objectives have been proposed:

1. To design a frequency controlled actuator
2. To integrate the actuator for drug delivery device
3. To characterize the wireless drug delivery device and IPMC actuator

1.5 Scope and Limitation of the Study

The performance of the wireless drug delivery device using IPMC microactuator will be evaluated in terms of its time response and deflection.

CHAPTER 2

LITERATURE REVIEW

2.1 Background Study

The IPMC artifice muscle or bending property was first discovered by Shahimpoor and Ogura in 1992 (Nikhil and Won-jong, 2004). Under a research on the application of IPMC as hydrogen pressure transducer, he notices the transduction of an IPMC generates a voltage (Sia,and Chris). This discovery had brought the rise of the application of IPMC as sensor. Later in the same year, Ogura proposed the bending ability under an applied voltage which had open up a new path of for IPMC to be applied as actuator (Sia,and Chris).

The actuation of IPMC was further studied by Nemat-Nasser and Zamanihave in early of 20th century. A detail analysis about the actuation and sensing phenomena related to composition, processing, and microstructure of IPMC materials had performed in their studies (Sia,and Chris).

The studies done by Nemat-Nasser and Zamanihave had later become a fundamental to the lately research. In 20th century, numerous of research had developed to improve the performance of IPMC actuator such as fabrications method, thickness of the IPMC, and different type of control method. All of those effort currently was brought to the application of IPMC actuator in biomedical field especially targeted drug delivery system.

In the recent year, research team of University Dankook had successfully discovered a new method to fabricate IPMC actuator. A 3-deminsional preshaped form of IPMC actuator had via a thermal treatment process was successfully demonstrated (Dong-IK, 2012). This new fabrication method allows the shape of IPMC actuator become much more adjustable.

Market for the IPMC material is expected to be expend as currently IPMC actuator was attempt to incorporate with biomedical implantable device. The market

for IPMC in industrial field had already started as IPMC had applied in some industrial application such as stepper motor, micropump and robotic joint (Andrew and et.at., 2012). A number of application was also attempt to incorporate with IPMC but varies issue still haven't overcome as still consist a large space will need to be explored.

2.2 Ionic Polymer Metal Composite

Electroactive polymer (EAPs) is smart material that the change in size or shape is depend to electrical signal. EAPs usually classified into two types, electronic and ionic (Cohen, Sherrit, and Lih, 2001). Among these ionic polymer, Ionic Polymer Metal Composite exhibit artificial muscle behaviour under applied voltage.

The anion and the hydrated mobile cation is uniformly arranged at normal condition. When voltage or electric field is applied across the membrane, the mobile cation and water will move toward the cathode. Therefore, higher pressure will produce at cathode due to accumulation of water and cation compare to anode which have lower pressure as water molecules and mobile cation have moved away from that area. The difference between the pressure will lead to the deformation of the polymer, resulting actuation as shown in Figure 2.1.

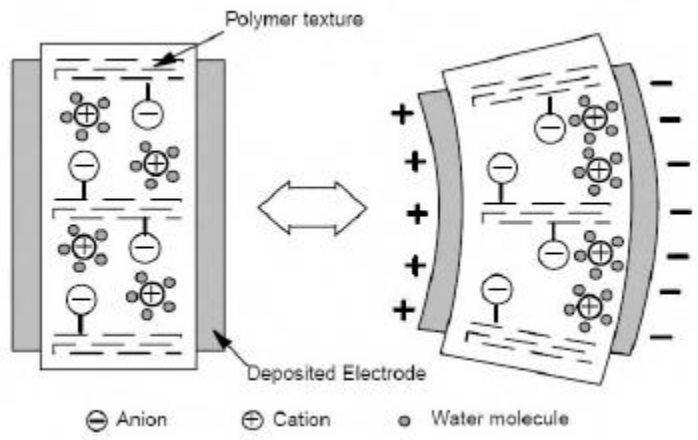

Figure 2.1: Operation principle of IPMC

IPMC commonly fabricated with Nafion (ionic exchange polymer) membrane and plated with a 10-20μm layer of platinum on the surface (Hubert and Leszek, 2015). In recent research, IPMC can operate best in humid environment and can be made as

self-contained encapsulated actuators to operate in dry environments as well (Younes, Sbeyti, and Jouni, 2009).

From the perspective of this research, IPMC actuator has the following advantages:

- Low actuation voltage (less than 5V)
- It can be use it micro size without loss in actuation properties
- Fast response
- Light weight

Most of IPMC research is focusing on material enhancement such as addition of carbon nanotube (Nguyen, et al., 2006), replacement of ionice liquid (Okamoto, Kikuchi, and Tsuchitani, 2010) and etc, in which there are lack of studied on the application on IPMC. Therefore, the drug delivery application of the IPMC will be the main subject of study in this thesis.

2.3 Load Carrying Capability of IPMC Actuator

As the voltage applied on the IPMC actuator from a fixed end to the free end is a constant, a constant distributed moment generated by electric field in any part of the actuator as in Figure 2.2 (Wang, Kwonn Cheng, 2008). Therefore, a constant distributed forces is applying on both sides of IPMC actuator from the fixed end to the free end which are equal numerically and opposite in direction (Wang, Kwonn Cheng, 2008).

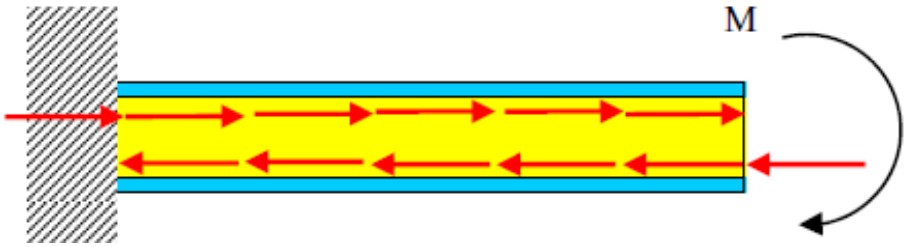

Figure 2.2: Force couple model for IPMC actuator

The generated force is depending on the applied voltage. This is because the applied voltage forced the charge to move along the ionic polymer (Mohamand O.Diab et.al, 2014). Force or load carrying capability of IPMC also relate to the area of it. An IPMC actuator with shorter length is more accurately with respect to the IPMC actuator with longer fingers (Mohamand O.Diab et.al, 2014).

The force generated by IPMC actuator usually does not extremely large due to its compliant nature (Deole and Lumia, 2006). However, for biomedical application especially those with micro-scale, this actually is an advantage because the objects will not be easily damaged or spoiled when handled by IPMC actuator (Deole and Lumia, 2006).

2.4 Wireless Implantable Drug Delivery Devices

Implantable systems are being utilised in biomedical devices since the integrated circuit technology was developed (Wise, et al., 2004). Wireless power transfer operated without the usage of batteries, is highly attractive in implantable device (Veeraiyah, et al., 2015). Many researches have been done using resonant magnetic induction coupling to operate implantable device. (Shyam, and Majid, 2014).

Wireless implantable drug delivery device (IDDs) allow drug to be delivered to the targeted region by controlling the external resonant magnetic field (Sarraf, Wong, and Takahata, 2016). To equip with biomedical competency, the material use for the actuator construction is always the main consideration. The material chosen should be biocompatible, stable and durable, and the ability of the material to control release of the drug (Todorova, et al., 2015).

Researchers have developed variety of wireless implantable drug delivery devices by taking advantages of various microactuator. Wang et al. demonstrated a compact IPMC actuated valveless pump for drug delivery. A wireless IDDs using shape memory polymer (SMP) microactuator was demostructed by Zainal and Mohamed Ali (Zainal, and Mohamed Ali, 2016). Sarraf, Wong, and Takahata demonstrated frequency selectable wireless IDDs using hydrogel micromachined resonant heaters (Sarraf, Wang, and Takahata, 2009).

The design of the drug delivery device can be classified into two type, one-time release based implantable drug delivery device and multiple-time release based implantable drug delivery device

2.4.1 One-time Release Based Drug Delivery Device

Wireless implantable drug delivery device with one-time release is a mechanism that the drug is completely release at one-time period using diffusion. The drug release is performed by breaking or opening the sealing membrane of the drug reservoir as shown in Figure 2.3. (Zainal, Mohamed Ali, 2016)

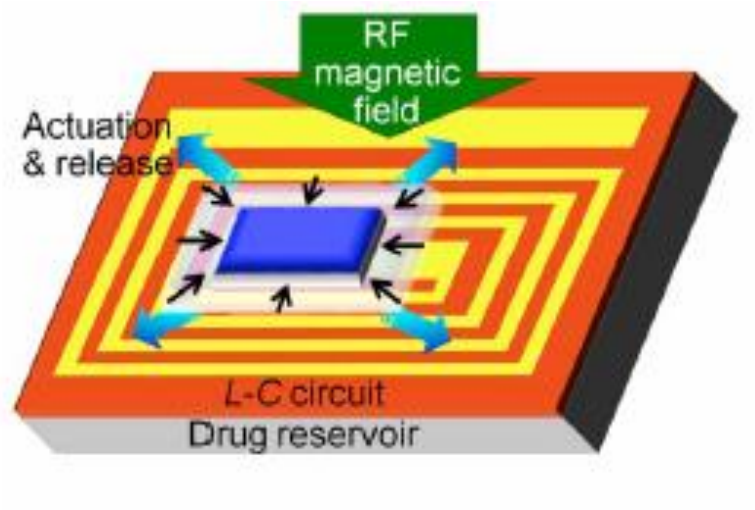

Figure 2.3: A frequency controlled wireless implantable drug delivery device using hydrogel microactuator

As shown in Figure 2.3, the drug inside the reservoir is sealed by the thermoresponsive hydrogel which use for actuation purpose. The *L*-*C* resonant circuit was designed as a heater which was wirelessly controllable by tuning the field frequency. The temperature arises when a field frequency is tuned to the resonant frequency of the device. Therefore, drug store inside the reservoir of the hydrogel is diffused out of due to the de-swelling of the material when the device temperature is increased (Sarraf, Wang, and Takahata, 2009).

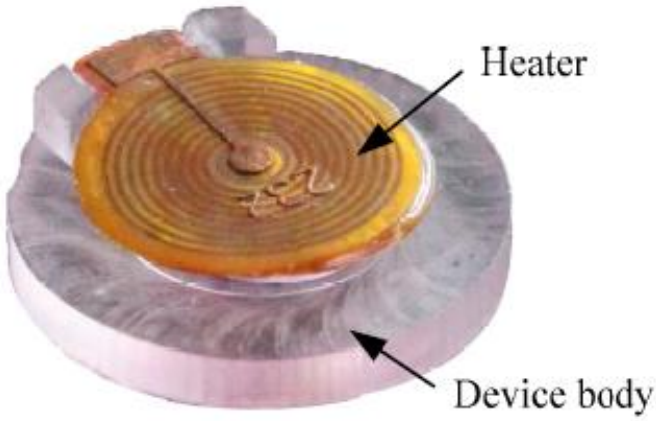

Figure 2.4: A frequency sensitive wireless SMP actuator

Figure 2.4 shown a wireless shaped memory polymer (SMP) implantable drug delivery device. The L-C resonant circuit was designed as a heater to control thermoresponsive SMP material. The heater temperature arises by tuning the field frequency to resonant frequency. As the temperature increase, SMP will turn into soft rubbery state and bend upward. Therefore, the drug store in the reservoir diffused out.

2.4.2 Multiple-Time Release Based Drug Delivery Device

Wireless implantable drug delivery device with multiple-time release operation enable multiple release of drug at several periods at applied pressure. The pressure is induced using micropump or microvalve as shown in Figure 2.5 and Figure 2.6 to push the drug out from the reservoir.

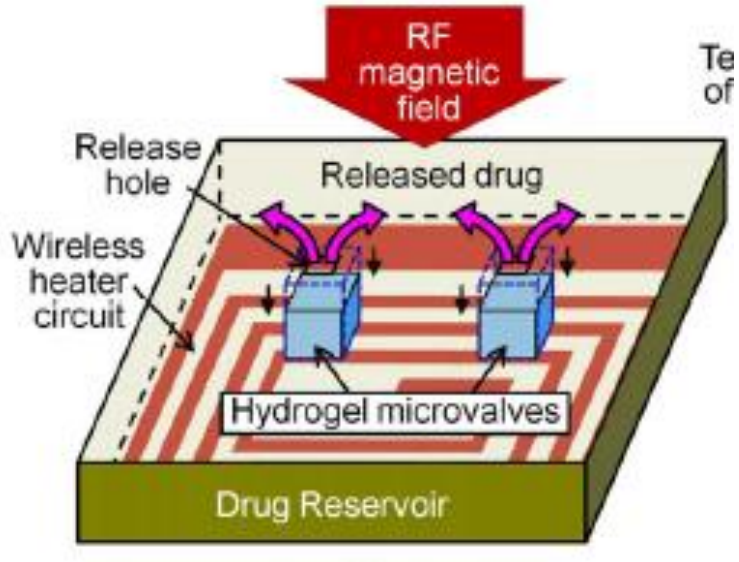

Figure 2.5: A wireless implantable drug delivery with hydrogel microvalves

As shown in Figure 2.5, the designed LC resonator circuit consist of wirelessly controllable heater and thermoresponsive hydrogel was selected as the microvalve material. By tuning the field frequency, the heater will be heat up and cause the shrinkage of microvalves to allow amount of drug to be released out from the release holes. When the resonant frequency is tuned away, it will stop the operation (Rahimi, and Takahata, 2011).

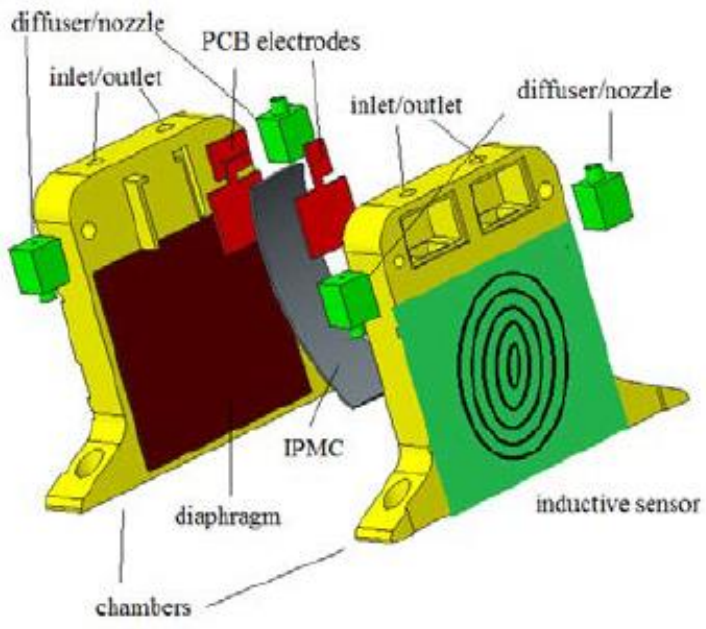

Figure 2.6: A IPMC actuated valvelss pump for drug delivery

As shown in Figure 2.6, a double-chamber valveless pump was actuated by cantilever IPMC. When voltage was applied, IPMC deflects and press the pump's diaphragm made of polydimenthysiloxane (PDMS). Therefore, drug distributed in the reservoir was pushed out by the pressure induced by the IPMC actuator. (Jiaqi Wang, and et al., 2016)

Numerous control method have been implemented and utilised to improve the controllability of the actuator to ensure the diffusion of drug under a constant rate. The size and shape of the reservoir for multiple-time release based unlike one-time release based design. The size and shape of the reservoir require a specific or special design to ensure the drug release in the desire dose and in mean time drug will not fully released.

2.5 Summary of Literature Review

Multiple-time release based wireless device allow require high repeatability of microactutor. For this research, ionic polymer is highly suitable for one time released operation due to the evaporation water molecules within ion the ion exchange membrane. To ensure repeatability of the actuator external controlled is required. For instance, an adaptive control system has been proven to be implemented for multiple time release operation to precisely control the displacement of the IPMC actuator to allow constant rate of diffusion (Andrew, 2012). This approach might further complicate the design of the drug delivery device. Taking the major objective of this research is to show the feasibility of IPMC in biomedical application into consideration, single release wireless drug delivery device appeared to be more appropriate candidate.

2.6 Related Theory

2.6.1 Resonant Frequency

Resonance is referring to an object that vibrate at natural frequency when a second object forces and eventually causing the second object vibrate. Every object consists of its own natural frequency and resonance frequency, referring to the matched natural frequency of two objects.

The resonant frequency coupling occurs only during 2 object share the same natural frequency. The maximum amplitude can be obtained at the resonant frequency as shown in Figure 2.7.

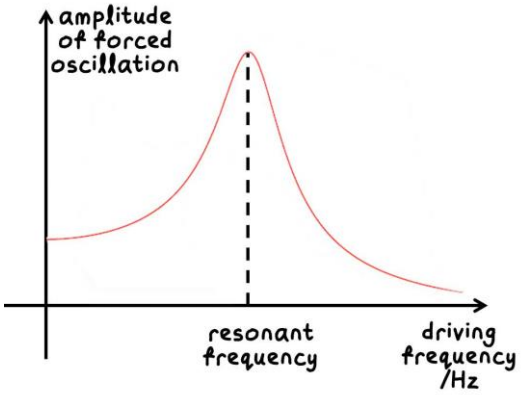

Figure 2.7: Resonant Frequency

Resonant frequency denotes as

$$frequency = \frac{1}{2\pi\sqrt{LC}} \tag{2.1}$$

where

L = inductance (H)

C = capacitance (F)

2.6.2 Magnetic Resonance Coupling (MRC)

Magnetic Resonance Coupling (MRC) enables a strong interaction of two object when within the same resonant frequency. A capacitor is added to the coils to allow it to obtain the natural frequency. Therefore, once the frequency of two coil is tuned to be the same, a strong interaction between two coils occur.

The conceptual view of MRC is shown in Figure 2.8.

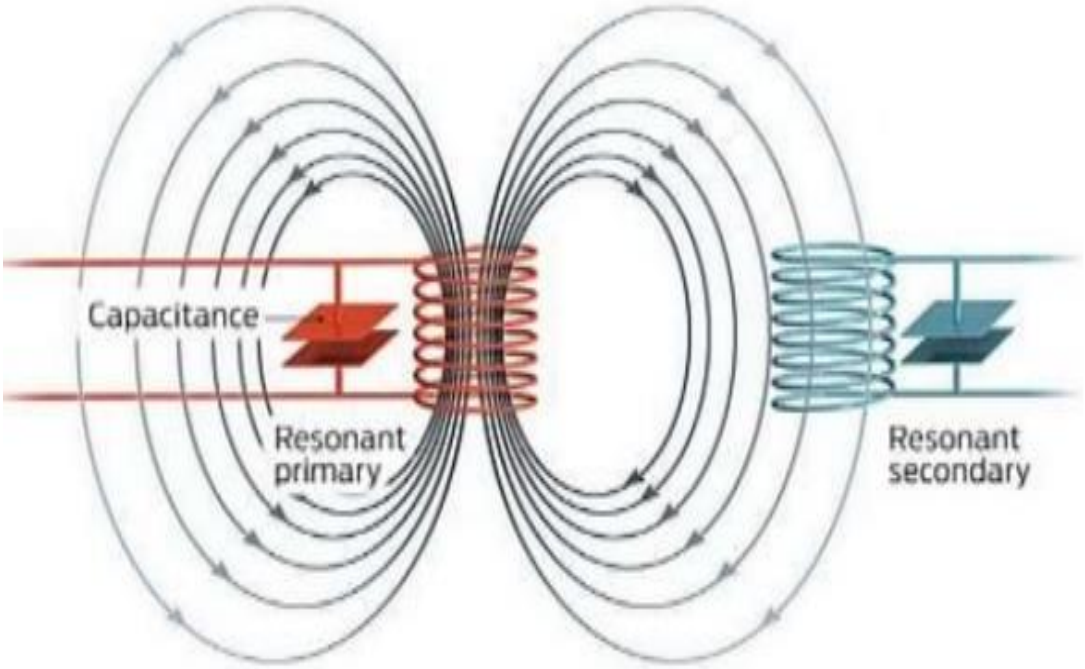

Figure 2.8: Conceptual view of Magnetic Resonance Coupling

CHAPTER 3

METHODOLOGY AND WORK PLAN

3.1 Design Scheme

The workflow for the frequency controlled IPMC microactuator for drug delivery is presented in Figure 3.1. The overall work plan can divide into research phase, designing phase, fabrication phase, testing phase and data collection phase as shown in Figure 3.1.

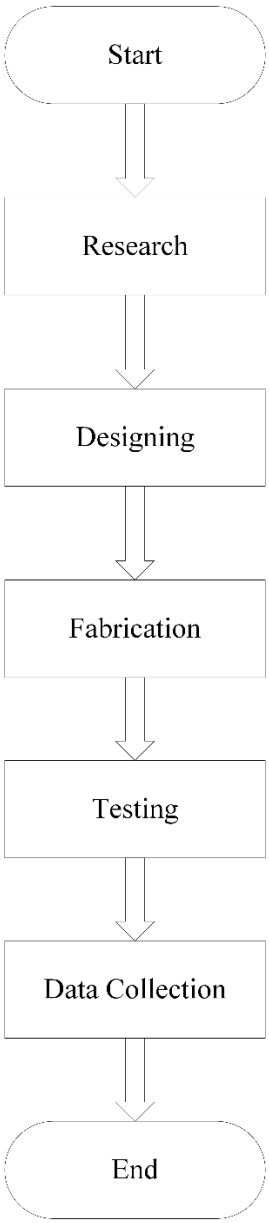

Figure 3.1: An overview of the project work plan

3.1.1 Design Phase

The planar *L-C* resonant circuit for transmitter and receiver, rectifier circuit, class-E amplifier, and device body were designed to ensure high efficiency of the transmitter and receiver. The overview of the workflow is shown in Figure 3.2.

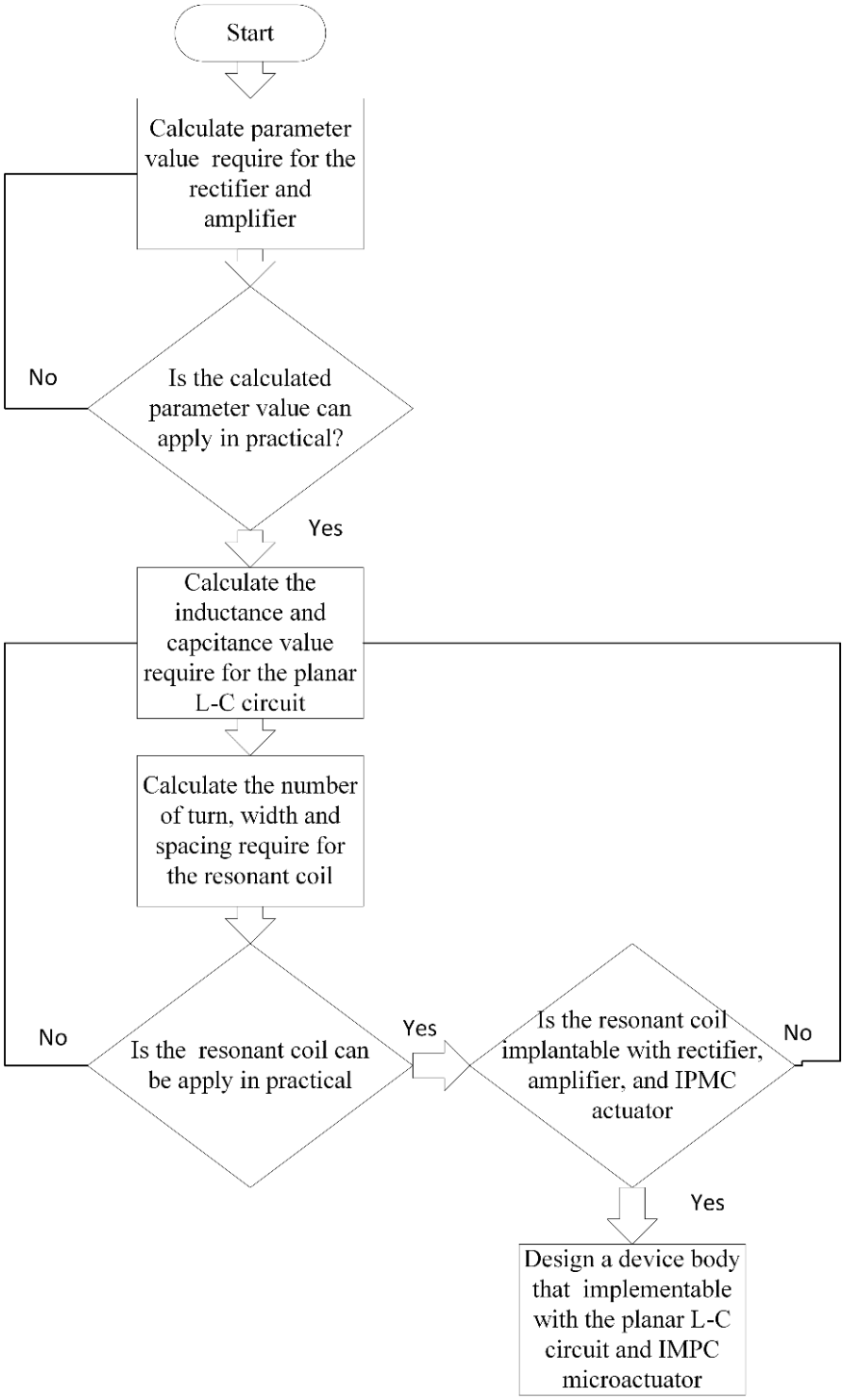

Figure 3.2: An overview of the workflow during design phase

3.1.2 Fabrication Phase

In this phase, planar *L-C* circuit, amplifier, rectifier, device body and IPMC microactuotor were fabricated. All the fabricated outcome was checked and tested to ensure that it was workable for future data collection. The overview of the workflow is shown in Figure 3.3.

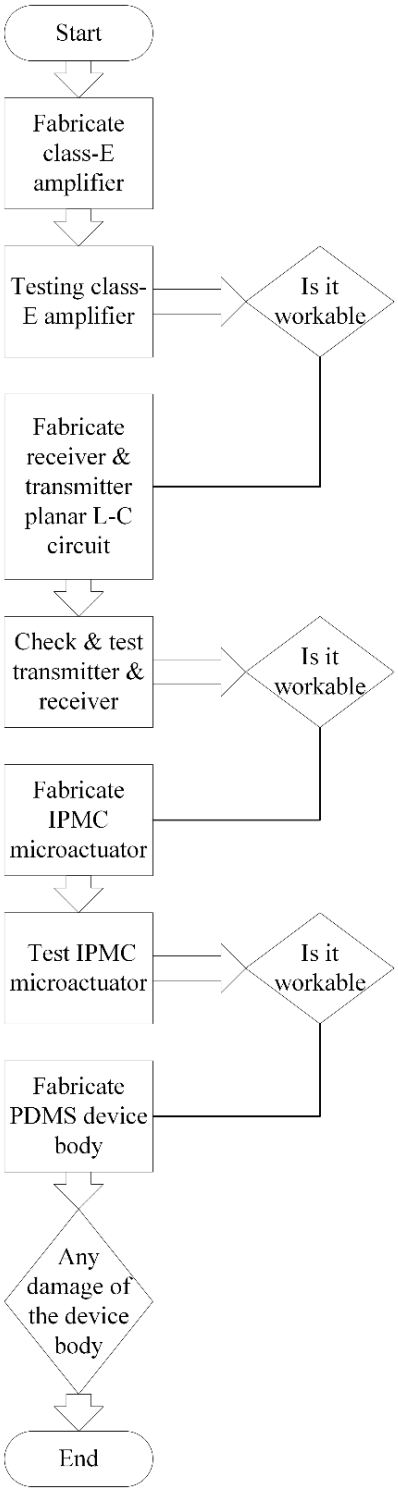

Figure 3.3: An overview of the workflow during fabrication phase

3.1.3 Data Collection phase

Lastly, several experimental methods were carried out to obtained the characteristic of the frequency controlled IPMC microactuaotor. Three set of data were repeated for each measurement. The overview of the workflow is shown in Figure 3.4 below.

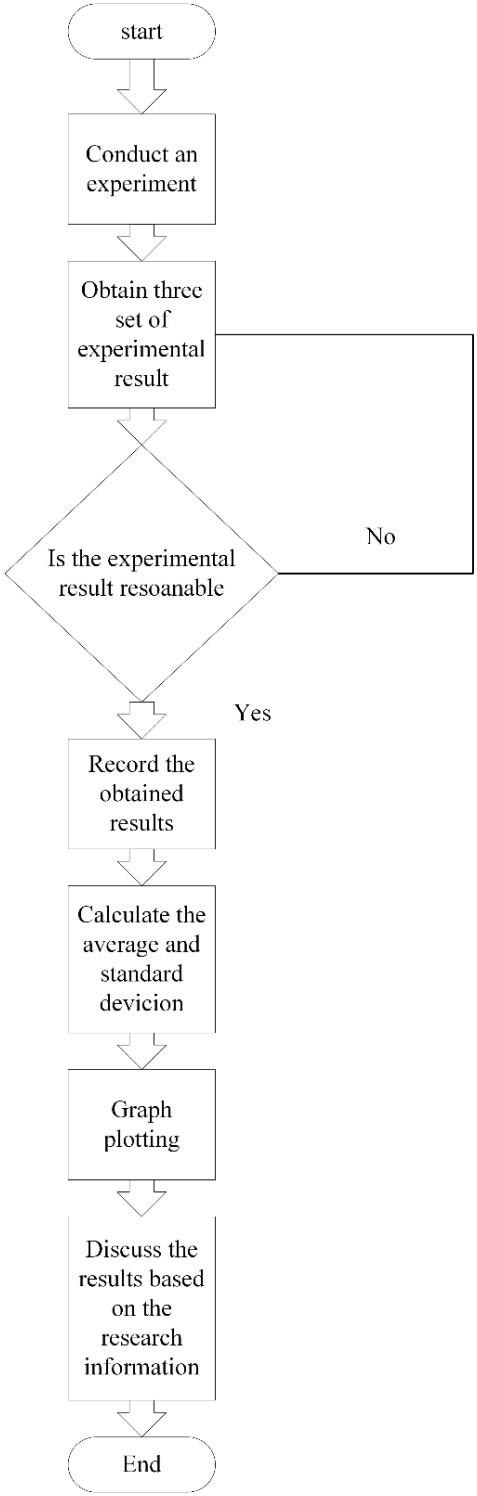

Figure 3.4: An overview of the workflow during data collection phase

3.2 Device Design and Working Principle

The drug delivery device utilizes magnetic coupling resonant transfer mechanism to transfer to transfer the power from transmitter to receiver wirelessly. A planar *L-C* receiver circuit was fabricated where the voltage induced at the receiver bends the EAP, IPMC when the field frequency, f_M is identical to the resonant frequency of the transmitter circuit, $2\pi f_r$. The efficiency of the power transfer is highly depending on the diameter of the transmitter coil.

The *L-C* resonant circuit essentially function as a wirelessly controllable power supply that can be adjusted simply by tuning the field frequency, instead of field intensity (Somayyeh, Ellie, Gregory, Kenichi, 2010). Therefore, this mechanism is potentially to be an accurate and reliable control mechanism for micromachined electroactive actuator. In particular, it offers an opportunity to implement drug delivery device for controlled delivery drug from reservoir.

This effort particularly targets microactuator that is wirelessly regulated the release of the drug store in the reservoir of the implanted device. The IPMC microstructure serves as the soft cover that use for sealing purpose. The purposed drug delivery device with frequency-controlled wireless IPMC microactuator is shown in Figure 3.5.

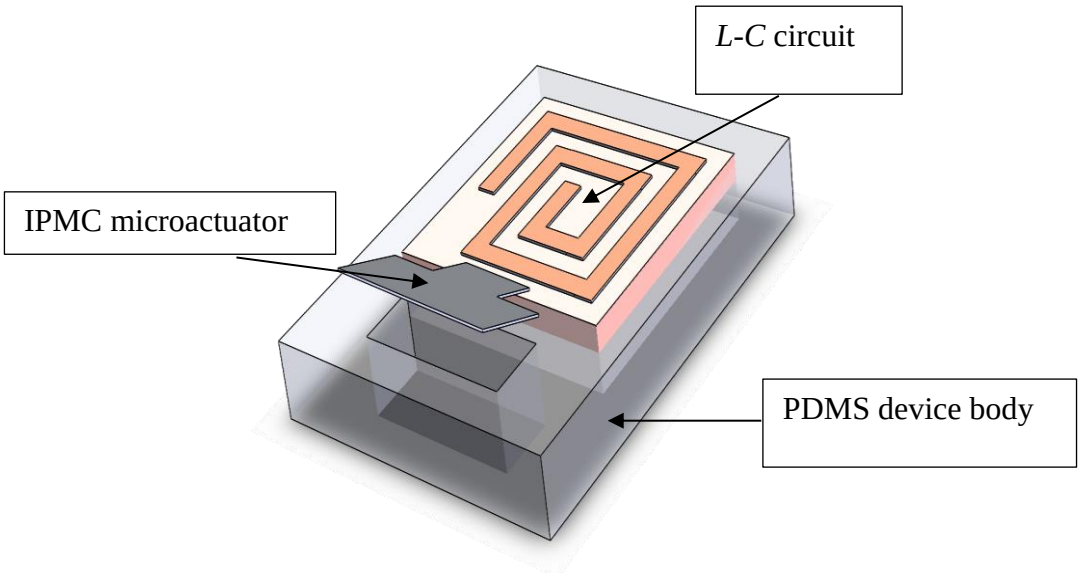

Figure 3.5: Drug delivery device with frequency-controlled wireless IPMC microactuator

To initiate drug release, the voltage is generated wirelessly through *L*-*C* resonant circuit. By field frequency tuning method, this cause the output voltage of the receiver *L*-*C* resonant circuit to increase and IPMC microactuator to bend upward, which unseal the reservoir to allow diffusion of drug from the reservoir.

An external class E amplifier will be attached to the transmitter to amplify the transmitting signal. In additional, to ensure the bending of IPMC in single direction, a rectifier circuit will also be attached to the receiver to convert the AC voltage to DC voltage. The schematic diagram for the proposed prototype drug delivery device with frequency-controlled wireless IPMC microactuator is shown in Figure 3.6.

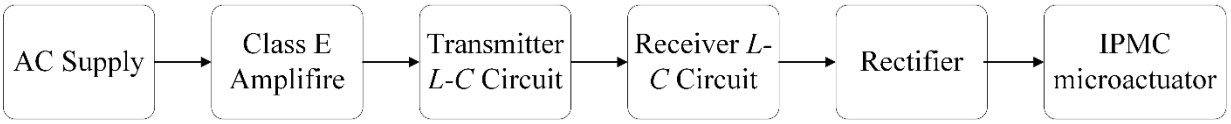

Figure 3.6: Block diagram of the wireless prototype drug delivery device with IPMC microactuator

3.3 Fabrication

3.3.1 Planar L-C circuit

The receiver planar L-C circuit is fabricated on one-side of the flexible PCB through PCB etching technique. Dry firm photoresists are used for all patterning process.

There are 4 types of coils planar design methodology which are was square, hexagon, octagonal and circular as shown in Figure 3.7.

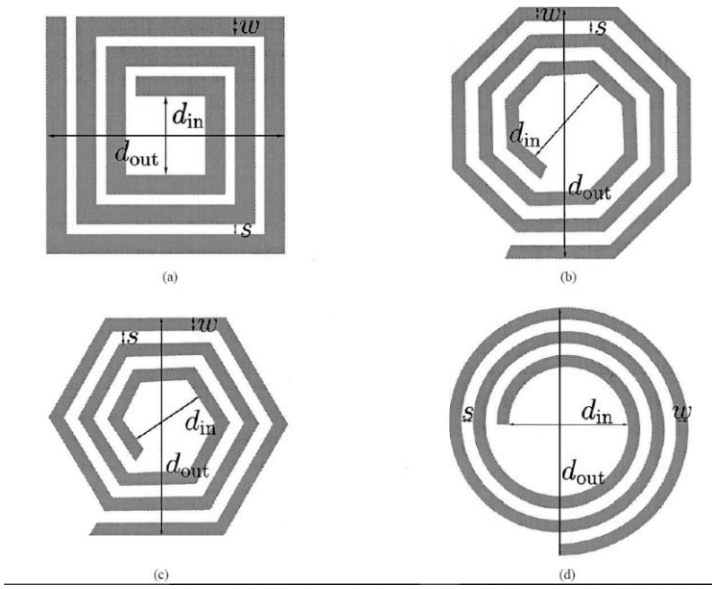

Figure 3.7: Concept view of the planar print spiral coil: (a) square (b) hexagon (c) octagonal (d) circular

The square planar print spiral coil shown in Figure 3.7(a) was selected for the planar L-C circuit. Mostly the coil is designed in circular shape but square planar print spiral coil chooses to simply the implement of the device. The resonator is in the outer loop and the load loop will fabricate in the inner loop and both is fabricated in same surface. Number of turn of the load loop need to be ensure small to allow the electromagnetic field in the resonator field to be maximise. The number of turn and the efficiency of the planar print spiral coil will vary according to the value of capacitance and inductance.

The characteristic values for the transmitter planar print spiral coil were obtained through following equation:

$$Frequency = \frac{1}{2\pi\sqrt{LC}} \tag{3.1}$$

$$L = K_1\mu_0\frac{n^2 d_{avg}}{1 + K_2\varphi} \tag{3.2}$$

$$d_{avg} = \frac{D_{out}}{D_{in}} \tag{3.3}$$

$$Fill\ factor, \varphi = \left|\frac{D_{out} - D_{in}}{D_{out} + D_{in}}\right| \tag{3.4}$$

Where

L = Inductancee

Dout = Transmitter Outer Radius,

Din = Transmitter inner Diameter,

D_{avg} = Average Diameter,

The inductance value for resonator loop of the transmitter can obtained via equation 3.1 and inductance for load loop of the transmitter can obtained via equation 3.2

The characteristic values for the receiver planar print spiral coil were obtained through following equation:

$$L = K_1\mu_0\frac{n^2 d_{avg}}{1 + K_2\varphi} \tag{3.5}$$

$$L = \frac{1.27\mu_0 n^2 D_{avg}}{2}\left(ln\frac{2.07}{\varphi} + 0.18\varphi + 0.13\varphi^2\right) \tag{3.6}$$

$$\text{Average Diameter}, d_{avg} = \frac{D_{out}}{D_{in}} \tag{3.7}$$

$$Fill\ factor, \varphi = \left|\frac{D_{out} - D_{in}}{D_{out} + D_{in}}\right| \tag{3.8}$$

where

L = Inductance

Dout = Transmitter Outer Radius,

Din = Transmitter inner Diameter,

D_{av} = Average Diameter,

The inductance value for resonator loop of the receiver can obtained via equation 3.5 and inductance for source loop of the transmitter can obtained via equation 3.6. Where C_n and K_n represent the coefficient expression and value of the coefficient for planar print spiral coil is shown in Table 3.1.

Table 3.1: Coefficient value of the planar print spiral coil

Layout	C_1	C_2	C_3	C_4	K_1	K_2
Square	1.27	2.07	0.18	0.13	2.34	2.75

The characteristic value of the transmitter and receiver is shown in table 3.4.

Table 3.2: Characteristics value of transmitter and receiver

Transmitter (100mm × 100mm)	(mm)
Capacitor, C	150pF
Resonator Outer Radius, D_{out}	100
Resonator inner Diameter, D_{in}	60
Average Diameter, d_{avg}	80
Number of turns, n	3
Width, $W_{resonator}$	5
Spacing, S	2.5
Capacitor, C	470pF
Source Outer Radius, D_{out}	54
Source inner Diameter, D_{in}	46
Average Diameter, d_{avg}	50
Number of turns, n	1
Width, W_{source}	4
Spacing, S	-
Receiver (11mm × 11mm)	(mm)
Capacitor, C	330pF
Resonator Outer Radius D_{out}	9.6
Resonator inner Diameter, D_{in}	2.2

Average Diameter, D_{avg}	5.9
Number of turns, n	8
Width, $W_{resonator}$	0.2
Spacing, S	0.3
Capacitor, C	2.2nF
Load Outer Radius, D_{out}	11
Load inner Diameter, D_{in}	10.2
Average Diameter, D_{avg}	10.6
Number of turns, n	1
Width, W_{loop}	3
Spacing, S	-

The transmitter and receiver were fabricated based on the calculated parameter values as shown in Table 3.2. The resonant frequency for the transmitter and receiver *L*-*C* resonant circuit is set as 13.56MHz due to the requirement of. The fabrication results are shown in Figure 3.8.

a.)

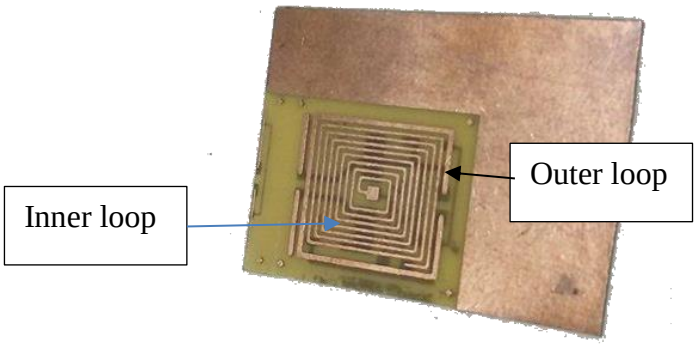

b.)

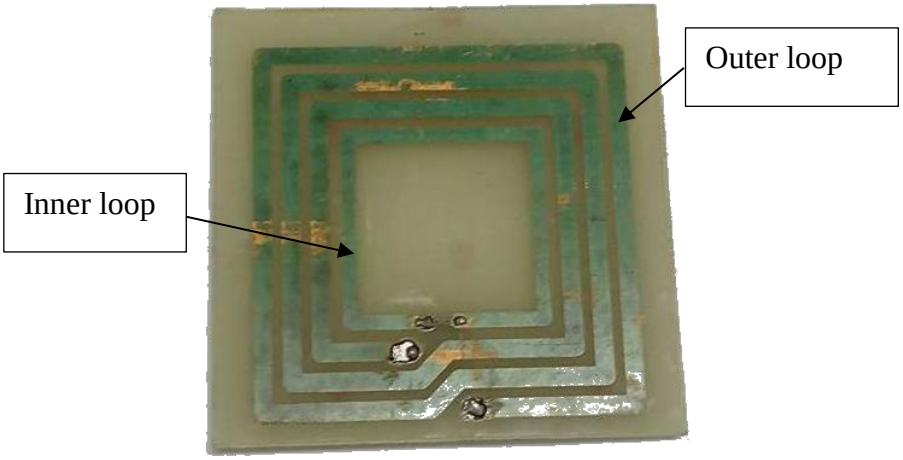

Figure 3.8: (a) Fabricated 11x11mm Receiver Planar *L-C* resonant circuit.
(b) Fabricated 100x100mm Transmitter Planar *L-C* resonant circuit.

3.3.2 Device Body

Variety of biomaterials such as polymeric materials have been selected to use as drug delivery carrier. However, not all materials are suitable for drug carrier. A material that suitable to developed in drug delivery device should have criteria such as chemical inertness, biocompatibility and minimum undesirable degradation by-products and possess suitable mechanical properties (Mashak, and Rahimi, 2009). Therefore, polydimethylsiloxane, PDMS was selected to develop the prototype device body.

The design of the device body and dimension value of the device body is shown in Figure 3.9.

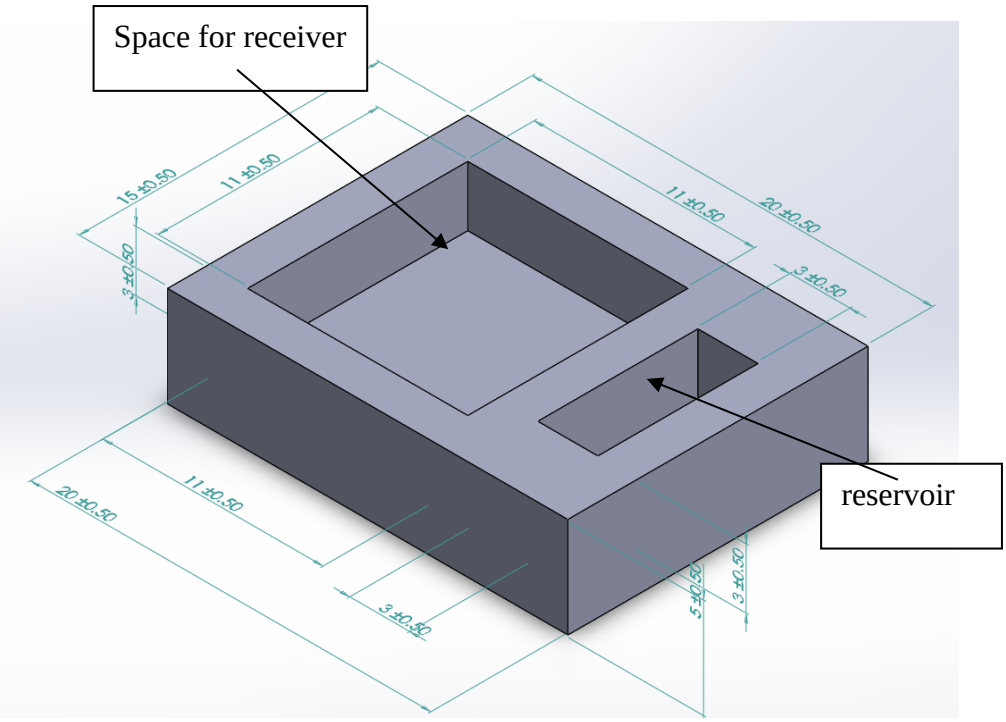

Figure 3.9: The dimension of the prototype IDDs device body

The total size of the prototype device body is designed with a rectangular shape of 20mmx15mmx5mm as shown in Figure 3.9 (W x L x H). The reservoir was designed with a rectangular shape with dimension 3mm x 8mm x 3 mm (W x L x H). A square shape with dimension 11mm x 11mm x 3mm (W x L x H) was designed to place the receiver. The spacing between the receiver and receiver is 2 mm. A transparent view of the design also shown in Figure 3.10 for a clearance view of the internal dimension.

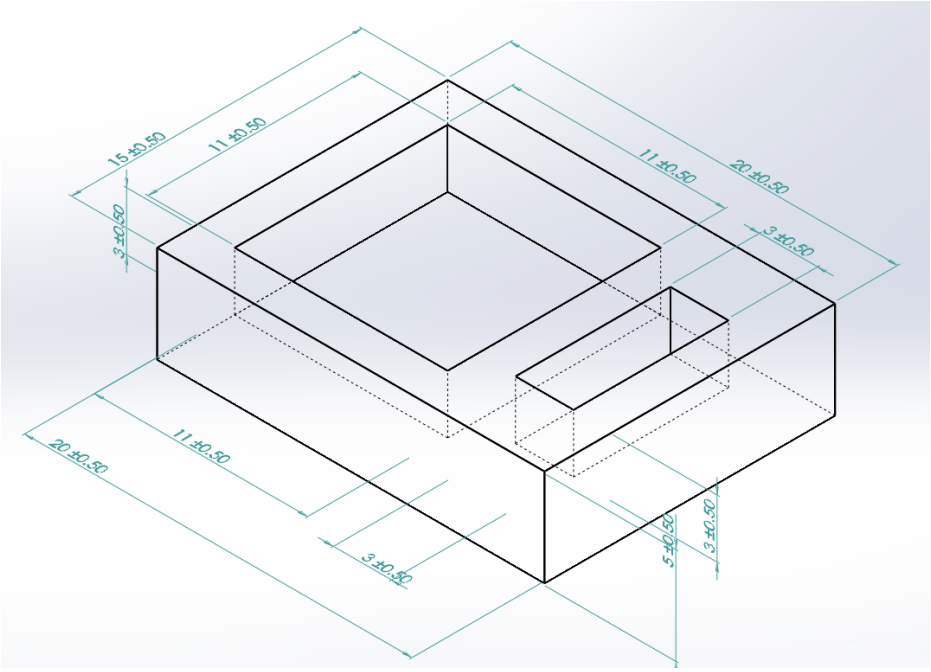

Figure 3.10: The transparent view of prototype device body

In order to obtained an ideal device body with accurate size and shape, a mould is created using resin based 3D printer as shown in Figure 3.11. It is essential to obtain a device body with precise dimension as to implement with the MCR-WPT system and IPMC microactuotor. The design and dimension of the mold is shown in Figure 3.12 and it transparent view is shown in Figure 3.13.

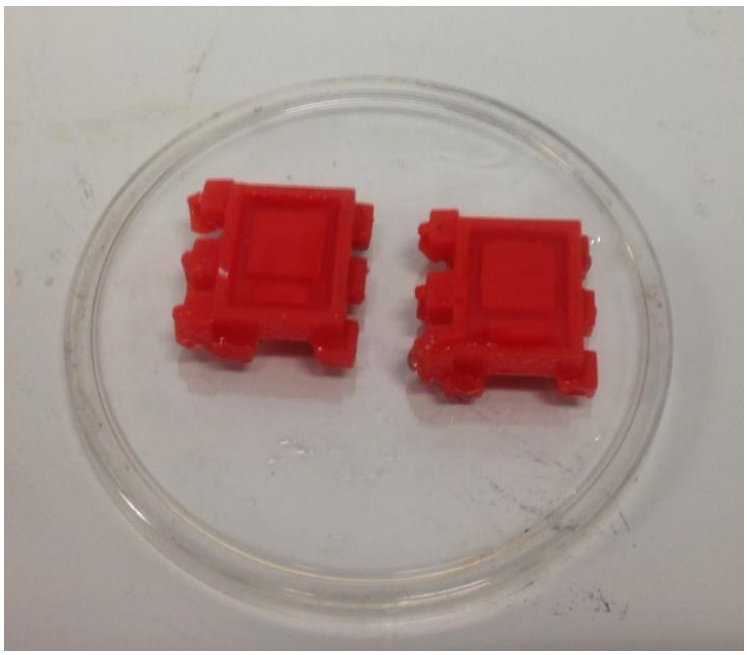

Figure 3.11: Mould created using resin based 3D printer

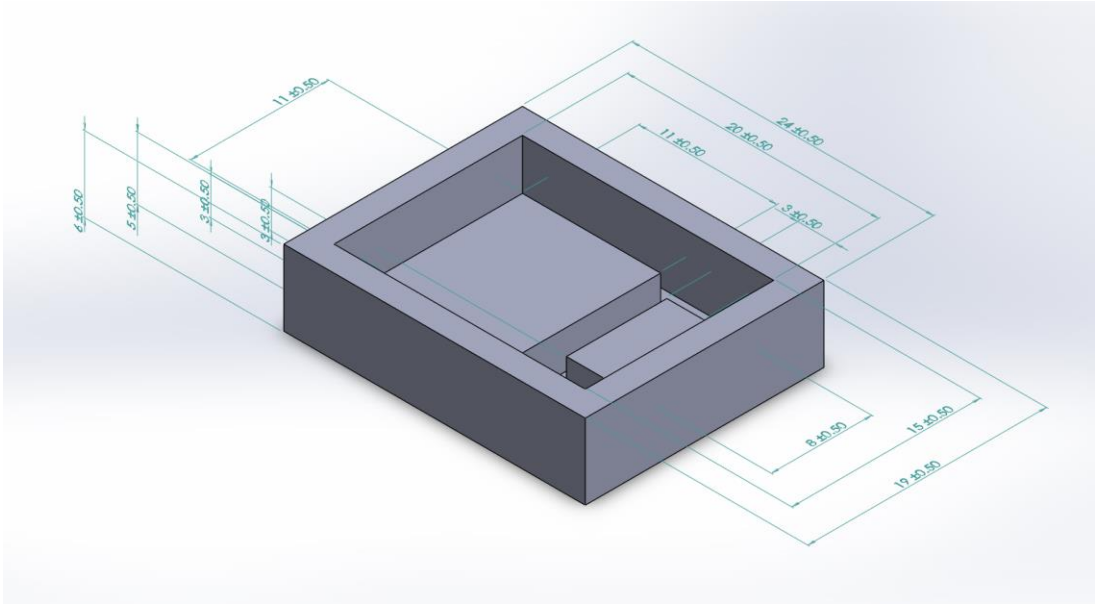

Figure 3.12: The designed mould of the wireless IDDs device

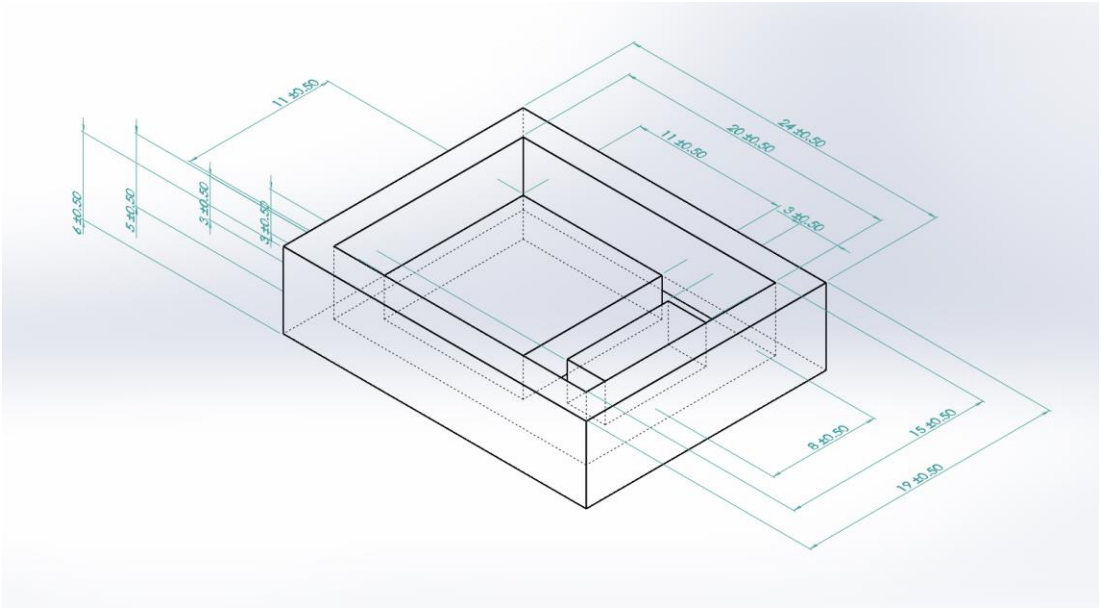

Figure 3.13: The transparent view of the designed mould

The PDMS mixed with a ratio of 10:1 PDMS monomer and curing agent with a glass rod prior pouring into the mould. The mould is fully filled with the PDMS; it was then put into a vacuum to degas the PDMS and remove the bubble for 15 minute. Lastly, PDMS was heated using hotplate with a 60ºC for 1 hour. After 1-hour of heating, the PDMS was removed. The fabrication result is shown in Figure 3.14.

Figure 3.14: Fabricated prototype device body using IPMC

3.3.3 IPMC Microactuator

In this effort, IPMC microactuator was fabricated with Nafion membrane through silver mirror process. The surface of the Nafion was first wiped with a sandpaper to remove dirt. This is to ensure the silver can be coated effectively on the Nafion surface and increase the conductivity of the IPMC. After that, Nafion is cut into desire T-shape with dimensions as shown in Figure 3.15.

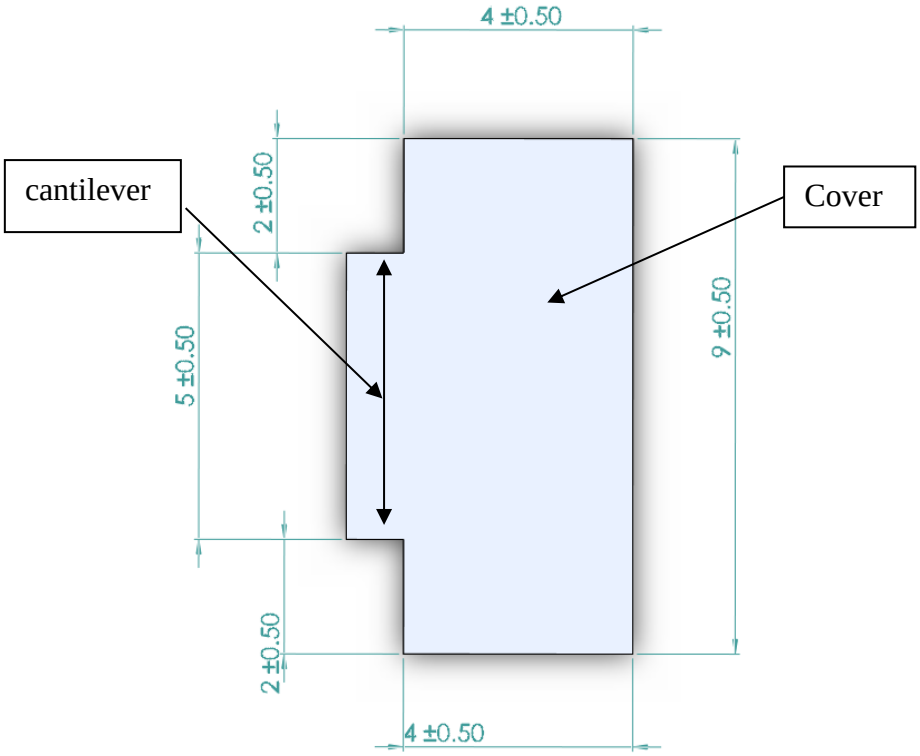

Figure 3.15: Dimension of the T-shape IPMC microactuator

The cantilever part of the IPMC microactuator as shown in Figure 3.15, portion of the surface for both side was furthered cover with a masking tape before undergo the silver mirror process to prevent the silver to be coated, ensuring polarity connection. Since the actuation was performed due to the movement of the positive ion to the cathode with the hydrated water molecules, which produce a volume change and bending motion toward the anode. Therefore, it is essential to make the top surface of the IPMC to be positive polarity and reverse side to be negative polarity to control drug release from the reservoir.

To fabricate the electrode, a mixture solution of ammonia, $AgNO_3$ with silver nitrate, NH4OH and a mixture solution of Glucose with sodium hydroxide, NaOH. The mixing ratio for these two solution is shown in Table 3.3. Nafion membrane was dipped into these two solution repeatedly at least 5 minutes to form a silver layer on the surface of the Nafion membrane. The complete fabricated IPMC microactuators are shown in Figure 3.16.

Table 3.3: Silver mirror process solution mixing ratio

Chemicals	Ratio	Concentration
AgNO3	1.2g + 60g(H2O)	1.9608 w/w %
NH4OH- 28% concentration	2g	
Glucose	0.8g	
NaOH	1.6g + 60g(H2O)	2.5974 w/w %

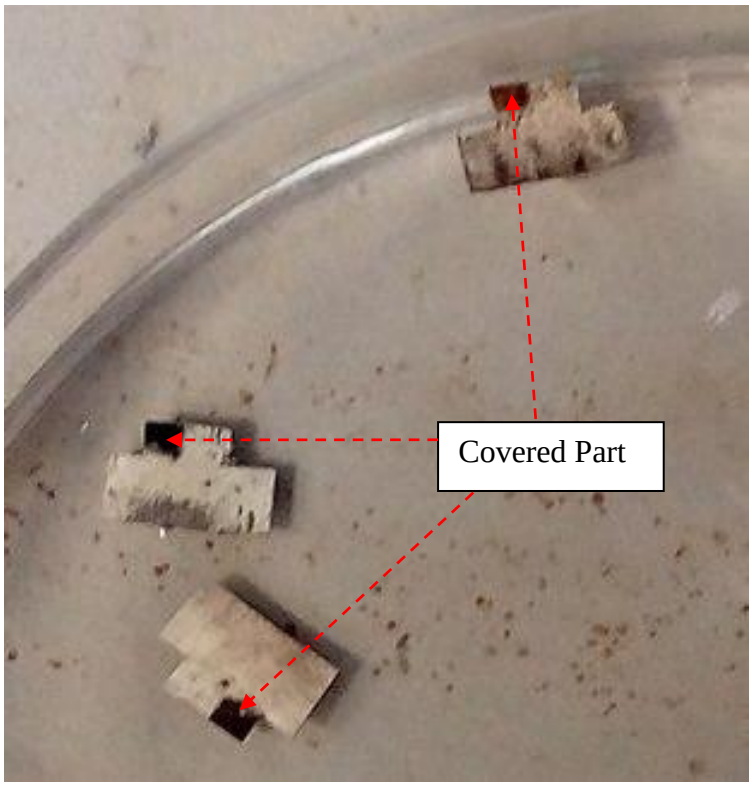

Figure 3.16: Complete fabricated IPMC microactuators through silver mirror process

3.4 Class-E Amplifier & Rectifier Circuit

As shown in Figure 3.2, a class-E amplifier and rectifier circuit were added to amplify the transmitted signal and convert the AC output voltage of the receiver planar LC circuit to DC voltage. In this chapter, the design principle of the class-E amplifier and rectifier circuit will be discussed.

3.4.1 Class E amplifier

Class-E amplifier provide promises high conversion efficiency and simple circuit design which lead to be highly promoted as frequency power source for MCP-WPT system. The schematic circuit diagram of Class-E amplifier is shown in Figure 3.17.

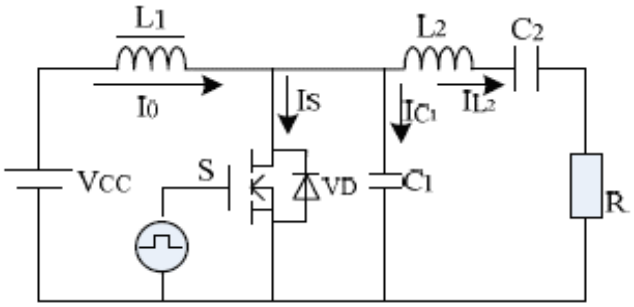

Figure 3.17: Schematic diagram of the class-E amplifier

According to the Raab condition, when the impedance angle of filter branch, φ = 49.052º, class E amplifier will then operate in best condition (Zhenya, Xuemei, and Bo, 2015). By using formula expressed in equation 3.9, 3.10, 3.11 and 3.12 all the characteristic value of inductance and capacitance that requires for the class E amplifier can be calculated.

$$Filter\ Inductance, L_2 = \frac{QR}{\omega} \tag{3.9}$$

$$Filter\ Capacitance, C_2 = \frac{1}{\omega(\omega L_2 - R\tan\varphi)} \tag{3.10}$$

$$Shunt\ Capacitance, L_2 = \frac{1}{\left(1+\frac{\pi^2}{4}\right).\pi.(\omega)(R)} \tag{3.11}$$

$$Choke\ inductance, L_1 = \frac{10}{\omega^2.C_1} \tag{3.12}$$

Where ω = angular resonant frequency (rad/s)

Q = quality factor

The calculation is performed by taking assumption at below and the calculation result is shown in Table 3.4 and 3.5.

Resonant frequency, f_r =13.56MHz

Quality factor, Q = 10

Resistance, R = 50Ω

Impedance angle of filter branch, φ = 49.052º

Remark: The resonance frequency of 13.56MHz is standard for biomedical device

Table 3.4: Calculated characteristic value for class E amplifier

Component	Parameter Value
Filter Inductance, L_2	5.87µH
Filter Capacitance, C_2	26.53pF
Shunt Capacitance, L_2	43.10pF
Choke inductance, L_1	31.96µH

Table 3.5: Proposed characteristic value for class E amplifier

Component	Parameter Value
Filter Inductance, L_2	5.70µH
Filter Capacitance, C_2	22.00pF
Shunt Capacitance, L_2	44.00pF
Choke inductance, L_1	47.00µH

The class E amplifier was fabricated on PCB board through soldering technique with the proposed component value as tabulated in Table 3.5. The fabrication result is shown in Figure3.18.

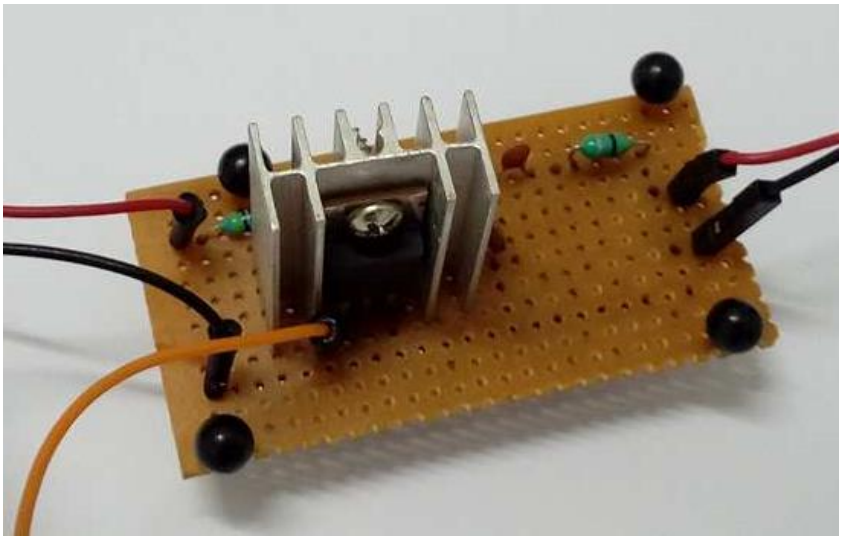

Figure 3.18: Fabricated Class-E Amplifier

3.4.2 Rectifier Circuit

A rectifier circuit was fabricated on the reserves side of the rectifier planar L-C circuit. Schematic diagram of the rectifier circuit is shown in figure 3.14.

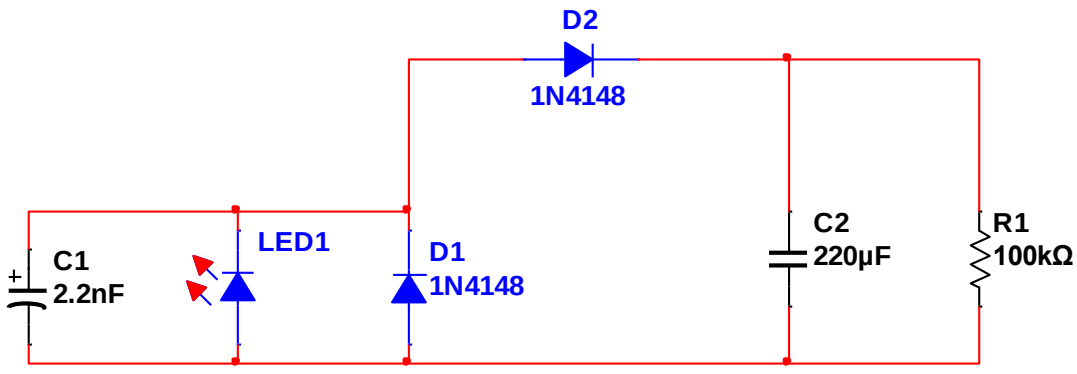

Figure 3.19: Schematic Diagram of the Rectifier Circuit

Remark: The capacitor C1 shown in Figure 3.19 is the capacitor for the load loop of the receiver planar L-C resonant circuit.

The purposed characteristic value of the rectifier circuit is tabulated in Table 3.6.

Table 3.6: Proposed characteristic value for rectifier circuit

Component	Parameter value
Capacitor	220µF
Diode	1N4148
Resistor	100kΩ
LED	-

All the component use for the rectifier circuit is surface mounted configuration (smd) type to ensure size of the rectifier is small as to be fitted at the planar *L*-*C* circuit with total dimension of 11mm x 11mm.

The output of the receiver planar *L*-*C* circuit at the top-side was connected to the input of the rectifier circuit to convert the AC voltage to DC voltage. The connection between two side of the flexible PCB was formed by using silver paste technique. A hole was made at the connection point between the receiver planar *L*-*C* circuit and rectifier, then silver epoxy was used to fill up the hole and thus forming a connectivity between the two surface of the flexible PCB.

3.4.3 Summary of Methodology

The prototype device body was fabricated with polydimethylsiloxane (PDMS), a silicon-based organic polymer. The reasons to make the device body using PDMS is because the shape obtain ability which make the desire size and shape of the device can be obtain easily. Moreover due to it inert, non-toxic, and non-flammable characteristic make PDMS as the first choice as the device body material.

IPMC microactuator was fabricated in a T-shape in order to fully covered up the reservoir of the device. The T-shape IPMC actuator will connected to the output of the rectifier and hence the actuation of it will be controlled by the MCR-WPT system.

As short, a planar MCR-WPT drug delivery device with a 50 x 50 mm transmitter and 11mm x 11mm receiver was fabricated with PCB acid etching technique and further implemented with IPMC microactuator. The wireless transfer efficiency and the IPMC microactuator characteristic were studied.

CHAPTER 4

RESULTS AND DISCUSSION

4.1 Wireless Drug Delivery Device Using IPMC Actuator

In this chapter, a wireless drug delivery device prototype with planar MCR-WPT system and frequency controlled IPMC microactuator was demonstrated and studied its characteristics were studied. The transmitter and receiver were fabricated in square loop to simplify the implementation of receiver with the device body. Therefore, it is essential for the receiver and transmitter to be fabricated in a square print spiral coil design on a PCB. A rectifier circuit was fabricated at the back side of the receiver planar L-C circuit to convert the output AC voltage to DC voltage to actuate the IPMC microactuator.

Experiment had performed to studied the characteristic of the device prototype. The results will be future discuss in this chapter.

4.2 Resonance Response & Distance Response of the MCR-WPT Prototype

The proposed drug delivery device controlled release from the drug reservoir of the device with IPMC microactuator that is actuated with the output DC supply from the receiver. Therefore, it is essential to determine the frequency response of the receiver and obtain the resonant frequency between receiver and transmitter to optimize the device performance. The experimental set up is shown in Figure 4.1(a).

The distance between the receiver and transmitter was varied to determine the frequency The experimental set up is show as Figure 4.1(b).

a)

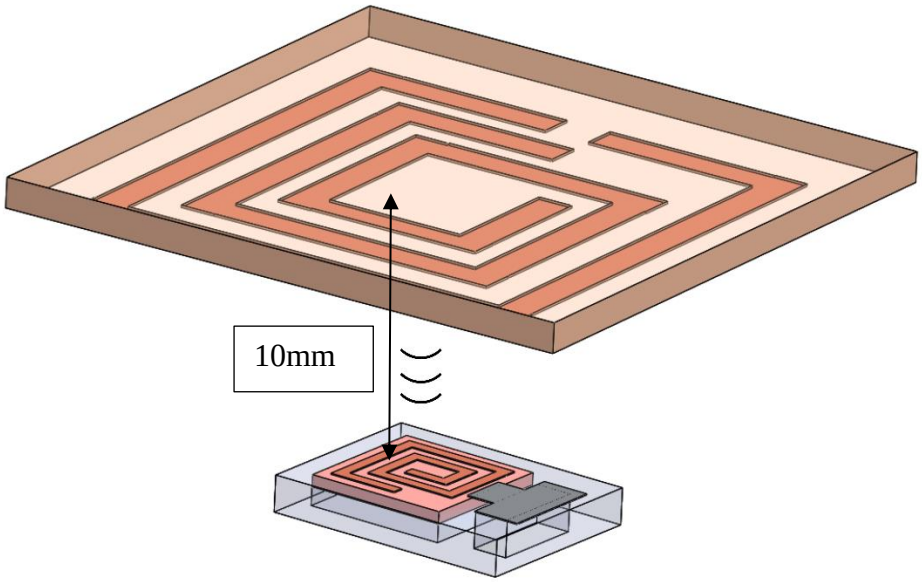

b)

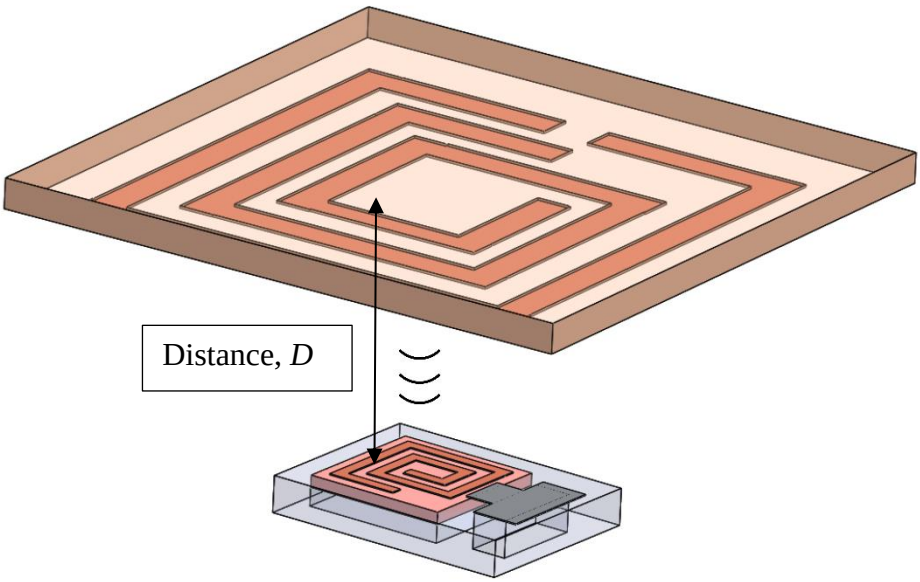

Figure 4.1: (a.) Experimental Setup For Resonance Response, (b.) Separation Distance, *D* Is Varied to Study Distance Response

4.2.1 Resonant Response

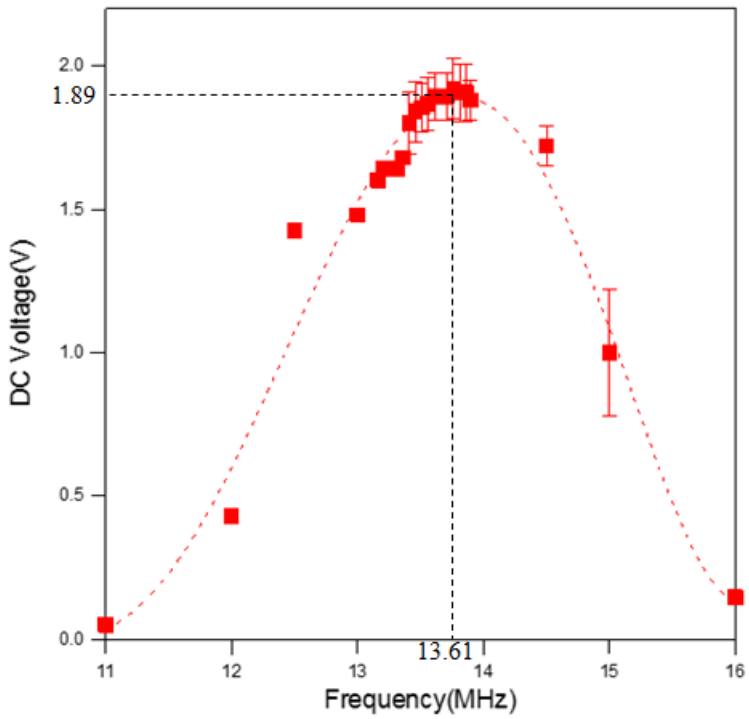

Figure 4.2: DC Voltage vs Field Frequency

The field frequency was tuned between the range of 11MHz and 16MHz and all the experimental results obtained was summarized in Table A-1. As shown in Figure 4.2, the optimise DC voltage obtained is 1.89V at frequency of 13.61MHz. Low voltage will be generated when the device is operated at non-resonance frequency. Therefore, the rate of drug release can be controlled by the tuning the frequency.

Table 4.1: Theoretical vs Experimental

	Theoretical	Experimental
Receiver Resonant tuned capacitor, nF	3.30	2.97
Receiver inductance, H	4.17×10^{-8}	4.60×10^{-8}
Resonant frequency, MHz	13.56	13.61
Error, %	<1%	

By comparing the theoretical and experimental results, it has less than 1% error due which may due to the 10% tolerance of the capacitor and the print spiral coil which fabricated with the etching technique.

4.2.2 Distance Response

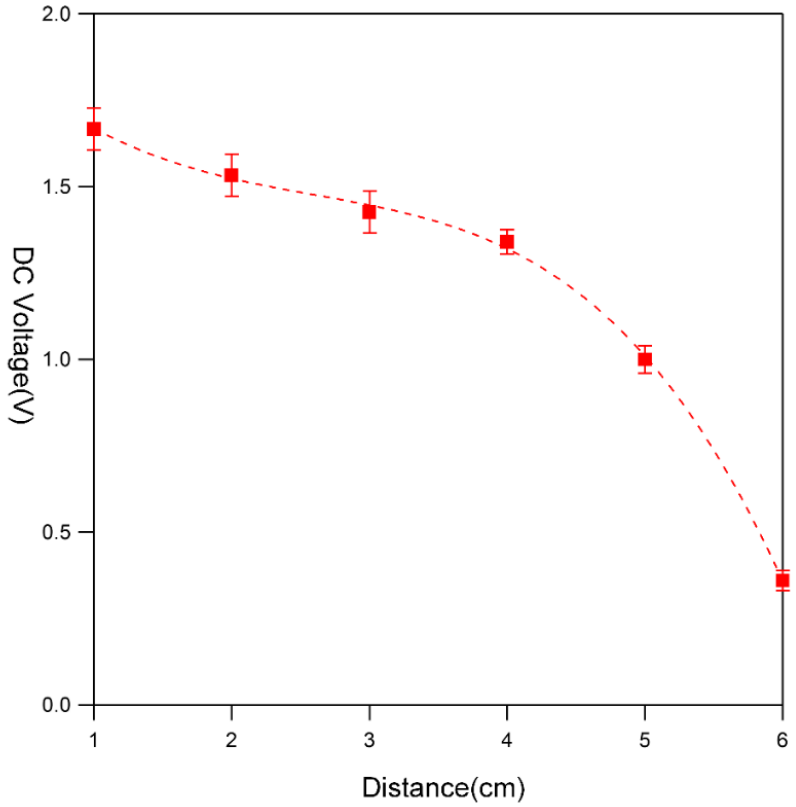

Figure 4.3: DC Voltage vs Separation Distance

Figure 4.3 shows the DC output voltage decrease as the separation distance between the receiver and transmitter and planar *L-C* receiver circuit increase. The IPMC operating voltage within 1 to 5 V range. Therefore, a maximum separation distance of 5cm can be achieved to ensure the workability of the device.

4.3 Effect on Asymmetrical MRC-WPT

To further characterize the prototype, the effect of the orientation angle to the output DC voltage was studied. It is known that the output of the receiver at different axial-alignment differ with orientation of the device in human body.

From section 4.2.2, the distance of the maximum DC output is 10mm at 13.61MHz. Therefore, the separation distance was fixed at 10mm and the angle between transmitter and receiver is alternated from 0º to 90º to study the effect of DC output voltage.

The experimental set up is shown in Figure 4.4 and the experimental results are shown in Table A-3.

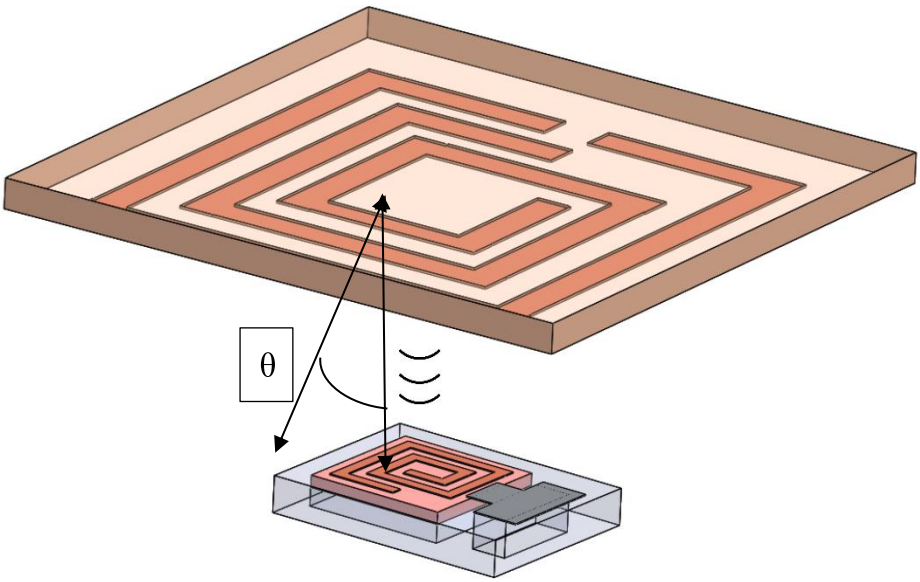

Figure 4.4: Asymmetrical Effect Experimental Setup

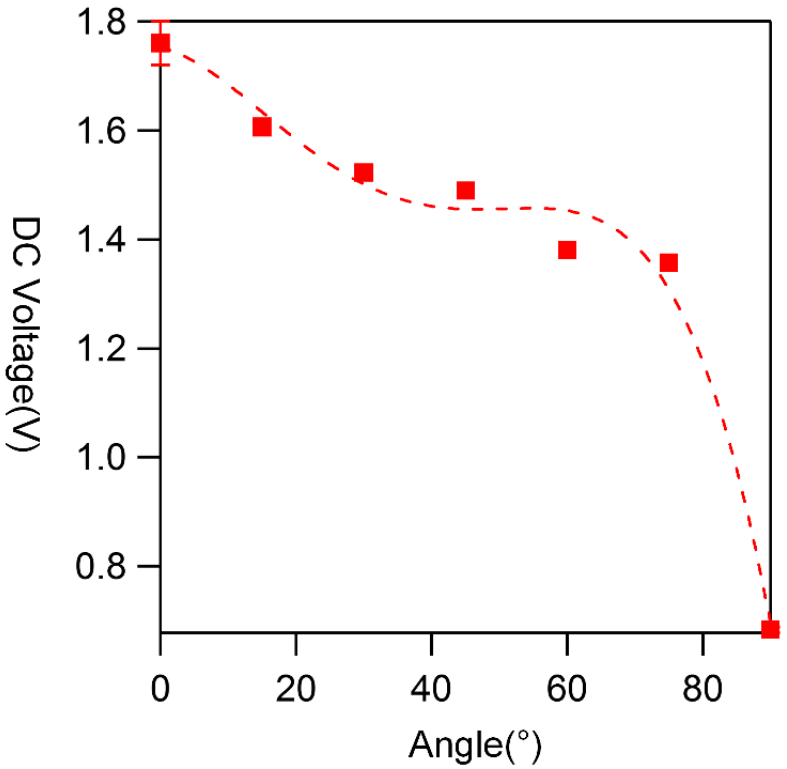

Figure 4.5: DC Voltage vs Angle of rotation

The angle of the L-C circuit orientation will affect the output DC voltage as can be seen from Figure 4.5, the DC output voltage decreases as the angle of orientation increases. At 0º angle, as the transmitter parallel to the receiver, the output DC voltage is the greatest because the magnetic coupling between the receiver and transmitter is strong and the magnetic field formed in a sphere cloud.

As the receiver move away from 0º angle alignment, the magnetic coupling between the receiver and transmitter become weak due to magnetic flux leakage. At 90º the receiver become perpendicular to the transmitter and hence output DC voltage is lowest.

4.4 Time response of the IPMC micro-actuator

In order to achieve proper operation of the IPMC microactuator, it is important to study how the IPMC microactuator deflects in response to changes of voltage and how fast can it responses. The experimental setup is shown in Figure 4.6.

The field frequency was set to be the resonant frequency, 13.61MHz and the separation distance between the receiver and transmitter was fix at 10mm to obtained the optimise DC output voltage. The device prototype was turn on for 20 seconds then turn off 20 seconds to observe the deflection and time response of the IPMC micro-actuator.

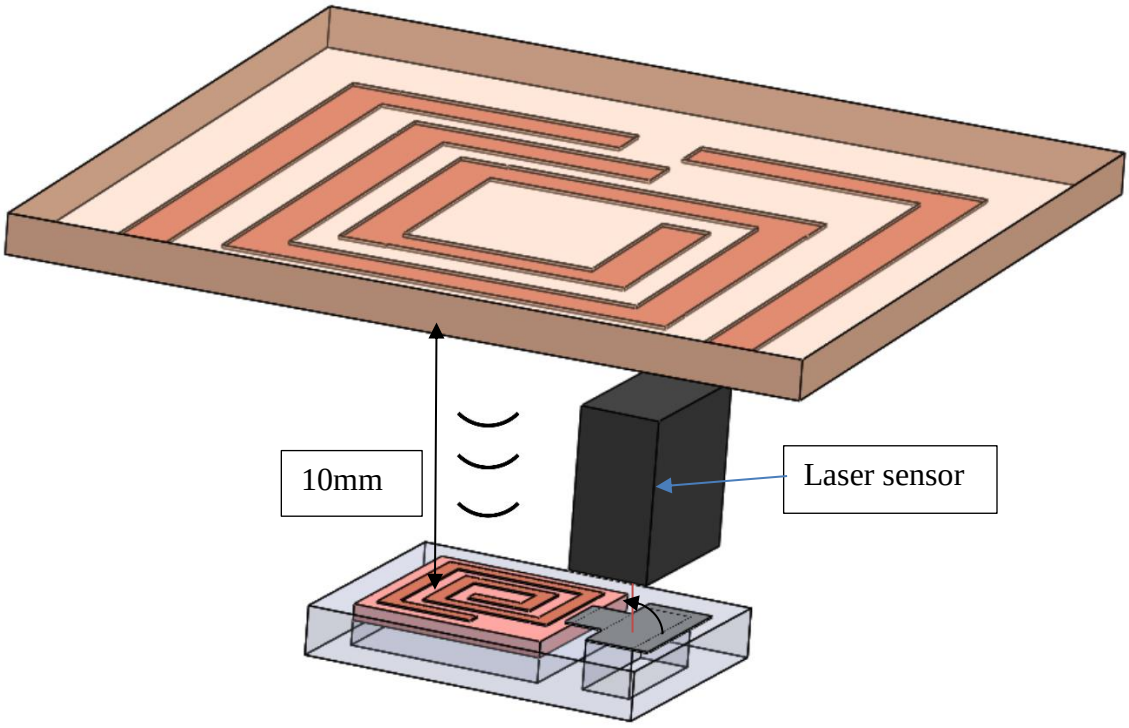

Figure 4.6: Time Response & Defection Experimental Setup

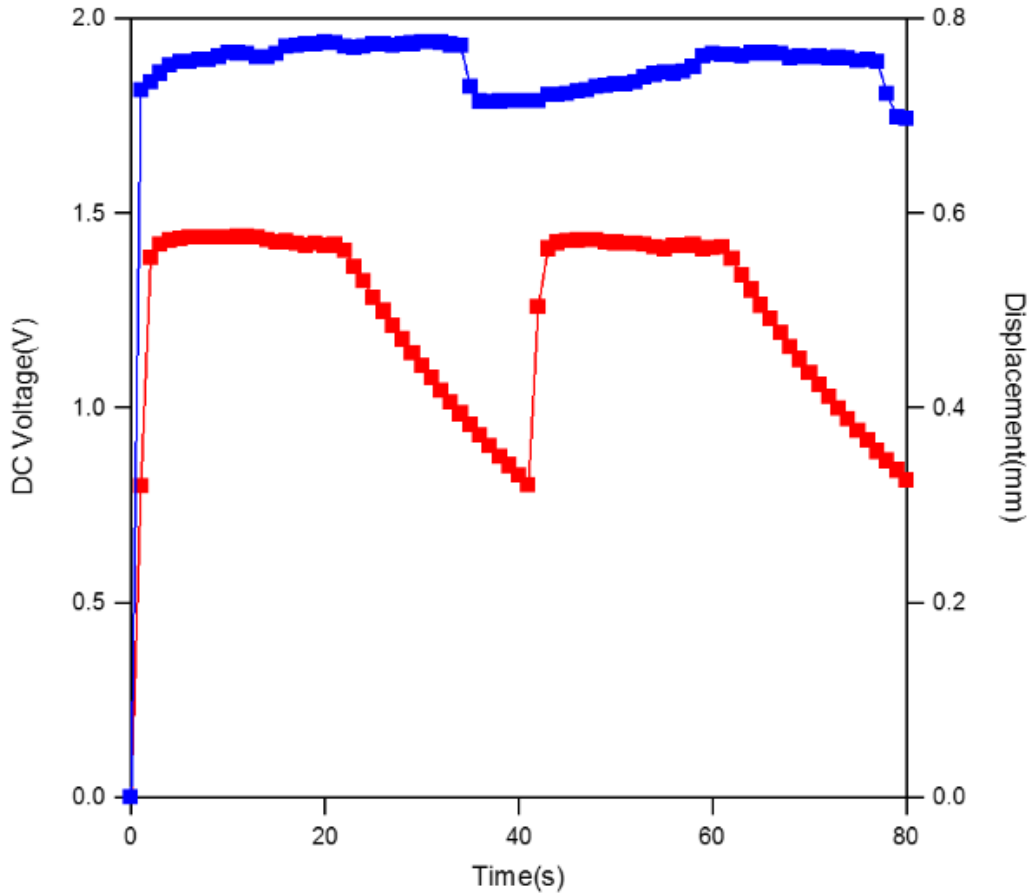

Figure 4.7: DC Voltage vs Deflection vs Time

Figure 4.7 depicts the IPMC microactuator is deflects faster during the turn on period compare to turn off period. This is because the deflection or bending of the IPMC is contributed by the movement of the cation and hence during turn off period it requires more time for the cation to move back it original location. Therefore, it is essential for the IPMC micro-actuator require more time to response during the turn off period.

Moreover, the highest deflection of the IPMC microactuator at first 20 second turn on period is noted at 0.77mm. However, for the highest deflection of the IPMC micro-actuator at second 20 second, the turn on period is noted with 0.76mm. The discrepancy of the deflection might be due to the loss of internal water molecule which require for the cation to have mobility.

CHAPTER 5

RESULTS AND DISCUSSION

5.1 Conclusion

This project presented a systematic study on controlled frequency IPMC microactuator for drug delivery device d prototype. A comparison on one time and multiple time release wireless drug delivery device were analysed in the literature review. The working principle of IPMC microactuator were also analysed. The proposed Magnetic Resonance Coupling, MRC and PDMS were chosen to be the wireless power transfer system and device body for the prototype device.

IPMC microactuator, an electroactive polymer which it deflection and time response were studied. The characteristics of IPMC microactuator were tested with MRC planar L-C circuit. IPMC miroactuator can response fast and actuation is affect by the voltage.

Planar L-C resonant circuit for transmitter and receiver PCB design were proposed to integrate MRC-WPT in a small system. The proposed size and shape of the planar L-C circuit were more easy to implement with biomedical device. The characteristic of the MRC-WPT such resonant frequency, transmission distance and axial-alignment were studied.

Furthermore, the device body were fabricated with PDMS due to its chemical inertness and biocompatibility. Amplifier and rectifier circuit also use to amplifier the transmission signal and make the conversion of AC to DC voltage.

5.2 Future Improvement

Lot of improvement can be done to optimize the proposed system such as adding an adaptive control element to control or improve the actuation of IPMC microactuator. Planar L-C resonant circuit also can direct implement at the IPMC actuator or device body to reduce the loss and enhance total power transferred.

REFERENCES

Sarraf, E., Wong, G. & Takahata, K., 2009. Frequency-selectable wireless actuation of hydrogel using micromachined resonant heaters toward implantable drug delivery applications. *TRANSDUCERS 2009 - 2009 International Solid-State Sensors, Actuators and Microsystems Conference*. 16 Jan.2017

Rahimi, S. & Takahata, K., 2011. A wireless implantable drug delivery device with hydrogel microvalves controlled by field-frequency tuning. *2011 IEEE 24th International Conference on Micro Electro Mechanical Systems*. 16 Jan.2017

Mostafalu, P. et al., 2015. Smart flexible wound dressing with wireless drug delivery. *2015 IEEE Biomedical Circuits and Systems Conference (BioCAS)*. 17 Jan.2017

Wang, Z., Wang, X. & Zhang, B., 2015. *A magnetic coupled resonance WPT system design method of double-end impedance converter networks with Class-E amplifier*. IECON 2015 - 41st Annual Conference of the IEEE Industrial Electronics Society. 23 Jan. 2017

Wang, J. et al., 2017. A Compact Ionic Polymer-Metal Composite (IPMC) *Actuated Valveless Pump for Drug Delivery*. *IEEE/ASME Transactions on Mechatronics*, 22(1), pp.196–205. 26 Jan.017

Aw, K.C. & Praneeth, S.V., 2013. *Low frequency vibration energy harvesting from human motion using IPMC cantilever with electromagnectic transduction*. *The 8th Annual IEEE International Conference on Nano/Micro Engineered and Molecular Systems*. 26 Jan.2017

Huei, S.G., Esa, M. & Kordesh, A., *RF spiral planar inductor designs - preliminary results [RFIC applications]*. *Asia-Pacific Conference on Applied Electromagnetics, 2003*. APACE 2003. 30 Jan. 2017

Mohan, S. et al., 1999. *Simple accurate expressions for planar spiral inductances*. *IEEE Journal of Solid-State Circuits*, 34(10), pp.1419–1424.

Zainal, M.A. & Ali, M.S.M., 2016. *Wireless shape memory polymer microactuator for implantable drug delivery aplication*. *2016 IEEE EMBS Conference on Biomedical Engineering and Sciences (IECBES)*. 5 Feb. 2017

Wisniewski, H. & Plonecki, L., 2015. *The dynamic properties of the IPMC polymer*. Proceedings of the 2015 16th International Carpathian Control Conference (ICCC). 7 Feb. 2017

Abdelnour, K. et al., 2012. *Wireless Powering of Ionic Polymer Metal Composites Toward Hovering Microswimmers*. IEEE/ASME Transactions on Mechatronics, 17(5), pp.924–935. 10 Feb. 2017

Nambiar, S.C. & Manteghi, M., 2017. A *simple wireless power transfer scheme for implanted devices*. 2014 United States National Committee of URSI National Radio Science Meeting (USNC-URSI NRSM). 18 Feb. 2017

Thangasamy, V. et al., 2015. *Wireless power transfer with on-chip inductor and class-E power amplifier for implant medical device applications*. *2015 IEEE Student Conference on Research and Development (SCOReD)*. 19 Feb.2017

Nemat-Nasser, S. & Thomas, C., Ionomeric Polymer-Metal Composites. *Electroactive Polymer (EAP) Actuators as Artificial Muscles: Reality, Potential, and Challenges, Second Edition*, pp.171–230. 4 Mar. 2017

Lin, Yi-Chen et al. "*An Ionic-Polymer-Metallic Composite Actuator For Reconfigurable Antennas In Mobile Devices*". *Sensors* 14.1 (2014): 834-847. Web. 7 Mar. 2017.

Wright, Jeremy C, and Diane J Burgess. *Long Acting Injections And Implants*. 1st ed. New York, NY: Springer, 2012. Print. 1 Apr. 2017

Bhat, N. & Kim, W.-J., 2003. *Precision Control of Force Produced by Ionic Polymer Metal Composite*. Design Engineering, Volumes 1 and 2. 12 Apr.2017

Mcdaid, A.J. et al., 2012. *Control of IPMC Actuators for Microfluidics With Adaptive "Online" Iterative Feedback Tuning*. IEEE/ASME Transactions on Mechatronics, 17(4), pp.789–797. 14 Apr.2017

Sarraf, E., Wong, G. & Takahata, K., 2009. Frequency-selectable wireless actuation of hydrogel using micromachined resonant heaters toward implantable drug delivery applications. *TRANSDUCERS 2009 - 2009 International Solid-State Sensors, Actuators and Microsystems Conference*. 15 Apr.2017

Deole, U. & Lumia, R., 2006. *Measuring the Load-Carrying Capability of IPMC Microgripper Fingers*. *IECON 2006 - 32nd Annual Conference on IEEE Industrial Electronics*. 22 Aug.2017

Diab, M.O. et al., 2014. *Electromechanical model of IPMC artificial muscle*. *2014 World Symposium on Computer Applications & Research (WSCAR)*. 22 Aug.2017

Wang, X.-L., Oh, I.-K. & Cheng, T.-H., 2008. *Mechanical model and analysis of ionic polymer metal composites biomimetic actuators*. *2008 7th World Congress on Intelligent Control and Automation*. 22 Aug.2017

Tsai, N.-C. & Sue, C.-Y., 2007. *Review of MEMS-based drug delivery and dosing systems*. *Sensors and Actuators A: Physical*, 134(2), pp.555–564. 22 Aug.2017

Wang, J. et al., 2017. *A Compact Ionic Polymer-Metal Composite (IPMC) Actuated Valveless Pump for Drug Delivery*. *IEEE/ASME Transactions on Mechatronics*, 22(1), pp.196–205. 24 Aug.2017

Bar-Cohen, Y., Sherrit, S. & Lih, S.-S., 2001. Characterization of the electromechanical properties of EAP materials. *Smart Structures and Materials 2001: Electroactive Polymer Actuators and Devices*. 24 Aug.2017

Okamoto, M., Kikuchi, K. & Tsuchitani, S., 2010. *Evaluation of operating characteristics of Flemion®-based IPMC with ionic liquids operated in water*. *2010 IEEE/SICE International Symposium on System Integration*. 26 Aug.2017

Nguyen, T.T. et al., 2006. *A Novel Polymeric Micropump based on a Multilayered Ionic Polymer-Metal Composite*. *IECON 2006 - 32nd Annual Conference on IEEE Industrial Electronics*. 26 Aug.2017

APPENDICES

APPENDIX A: Table

Table A-1: DC Voltage vs Field Frequency

Field Frequency, MHz	DC Voltage, V
11	0.05
12	0.43
12.5	1.43
13	1.48
13.16	1.60
13.21	1.64
13.26	1.64
13.31	1.64
13.36	1.68
13.41	1.80
13.46	1.84
13.51	1.85
13.56	1.87
13.61	1.89
13.71	1.89
13.9	1.88
14.5	1.72
15	1.00
16	0.15

Table A-2: DC Voltage vs Distance

Distance, cm	DC voltage, V
1	1.67
2	1.53
3	1.43
4	1.34
5	1.00
6	0.36

Table A-3: DC Voltage vs Angle of rotation

Angle of rotation, º	DC voltage, V
0	1.76
15	1.61
30	1.52
45	1.49
60	1.38
75	1.37
90	0.68